GPS ON THE RAILWAY

A STUDY OF THE VALUE OF INCORPORATING KNOWLEDGE OF THE TRACK IN A TRAIN POSITIONING SOLUTION

Alexander Parkins

MSc in Surveying

2004-5

UNIVERSITY COLLEGE LONDON

DEPARTMENT OF GEOMATIC ENGINEERING

ABSTRACT

The current capacity of the rail network is limited by the train positioning system employed. Trains are kept further apart than the minimum safe stopping distance because their positions are not known precisely. GPS offers a potential solution to this problem and would also allow a reduction in track-side positioning infrastructure and possibly even track-side signals, resulting in cost savings. However, the high reliability requirement for such a safety-critical application means that there are many problems that must be overcome before GPS is useable.

One of the most serious obstructions to the use of GPS stems from the nature of the railway; a considerable proportion of the network runs through cuttings, which reduce the number of visible of GPS satellites. In practice, there must be a minimum of five satellites visible at all times since error detection is essential for safety. This criterion is often not met in the presence of obstructions. We do however have an additional piece of information about the position of a train – we know it is located on the track. A technique is being developed in the UCL Department of Geomatic Engineering which incorporates knowledge of the track location into the positioning solution. This should improve precision and reliability as well as allowing a position with a minimum of three visible satellites. This project analyses the effectiveness of this technique by creating an Excel spreadsheet that computes both this 'Track Known' solution and the conventional 'Track Unknown' solution. This allows both the general quality of GPS positioning in a cutting and the benefits of the Track Known solution to be assessed.

Analysis of the spreadsheet reveals that location within Britain does not greatly affect the quality of position obtained, but the azimuth of the cutting creates significant variation. It is shown that high precision knowledge of the track makes little difference to the Track Known improvement, allowing the potential for good results with a low-precision and easily obtainable track database such as may be obtained from existing mapping sources. Steeper cutting sides are seen to significantly increase the benefit of the Track Known solution, but positioning still becomes unreliable as the cutting sides increase above 35°.

CONTENTS

1. INTRODUCTION

1.1 BACKGROUND

Positioning on the railway is currently achieved through the division of the track into sections of about 1 km, each of which may only contain a single train. The presence of a train in a given section causes a current to flow between the rails, enabling the control centre to determine which sections are occupied. This system guarantees a safe distance between consecutive trains, but is inefficient since this spacing may be further than the minimum required stopping distance. Currently, increasing the capacity of the railways means making trains longer rather than more frequent, which is not beneficial for passengers.

Positioning by GPS could improve the efficiency of the railway network because more precise knowledge of the location of trains would allow them to be run closer together whilst retaining safe minimum distances. This method could reduce maintenance costs due to a lower requirement for track infrastructure. Advanced applications might allow track-side signals to be replaced with a 'virtual signal' system, where instructions are transmitted to the driver via a screen in the cab.

A significant problem with the use of GPS for such an application is the necessity for at least five (to enable error detection) visible satellites to compute a position. In open terrain or on aircraft this is easily achievable, but railways often run through deep cuttings and tunnels for long stretches with the result of a loss of position for a significant period of time. This is obviously unacceptable in a safety-critical application.

A technique is being developed within the UCL Department of Geomatic Engineering which allows knowledge of the location of the track to be included in the positioning solution. This is useful for trains (since we know the train is always on the track) and also has applications for other vehicles that are restricted to travel along known lines, e.g. vehicles along roads. This technique should allow a solution to be computed with a minimum of two satellites (three for error detection) and increase the precision and reliability of the position thus obtained.

1.2 PROJECT AIM

The aim of this project is to determine the benefits to GPS positioning in a railway cutting of including knowledge of the track in the least squares solution. 'Track Known' and 'Track Unknown' solutions will be compared for different cutting azimuths, locations, side slopes and track precisions.

1.3 PROJECT OUTLINE

An Excel spreadsheet will be developed to generate appropriate data to make such comparisons. This report will consist of a description and analysis of the spreadsheet, which has been submitted electronically alongside it.

After some initial discussion (chapter 2), the inputs and outputs of the spreadsheet are described (chapter 3), followed by an explanation of the calculations used in the spreadsheet (chapter 4). The solved and unsolved problems encountered are then discussed (chapter 5) and the spreadsheet is tested against simulated and real data (chapter 6). The results of the spreadsheet are then analysed and conclusions drawn about the usefulness of the Track Known solution (chapter 7). Finally, suggestions for further work are presented (chapter 8).

2. INITIAL DISCUSSION

This chapter details issues surrounding the construction of the spreadsheet.

2.1 UTILISING KNOWLEDGE OF THE TRACK

2.1.1 OVERVIEW OF THEORY

The theory behind the technique for including knowledge of the track into the least squares adjustment is outlined below.

The track is broken down into a series of straight lines, each defined by the co-ordinates of two end points. We know the train is restricted to the track and can determine on which segment it currently lies by extrapolating from previous positions. This information can be included in the positioning solution by projecting the equation of the current track line to two planes, initially the X-Y and X-Z planes, as illustrated by figure 2.1 (see section 5.1.1 for discussion). Each projected line gives one equation in the least squares formulation, so knowledge of the track gives two additional equations.

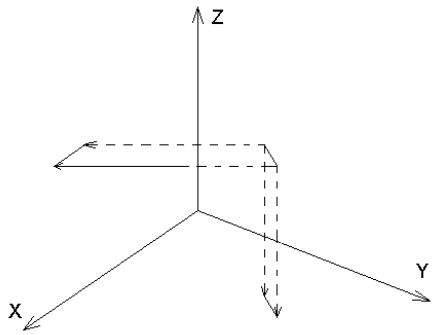

Figure 2.1: Projection of Track onto X-Y and X-Z Planes

2.1.2 TECHNIQUES FOR INCORPORATING KNOWLEDGE OF THE TRACK INTO LEAST SQUARES

This section describes the process followed during the course of developing the theory outlined in 2.1.1 for inclusion in the least squares positioning solution.

(i) **Track Line as Observation Equations**

The formulation of the least squares equations is the same as for Track Unknown, but each projected line is included as an additional observation.

The projected lines give two functional equations:

$f_1\left(X_p, Y_p, Z_p, \Delta t\right) = Y_P - m_1 X_p - c_1$, and

$f_2\left(X_p, Y_p, Z_p, \Delta t\right) = Z_P - m_2 X_p - c_2$.

where $m_1 = \dfrac{Y_2 - Y_1}{X_2 - X_1}$, $m_2 = \dfrac{Z_2 - Z_1}{X_2 - X_1}$, $c_1 = Y_1 - m_1 X_1$, $c_2 = Z_1 - m_2 X_1$.

X_1, Y_1, Z_1, X_2, Y_2 and Z_2 are fixed parameters.

These two observation equations can be linearised and included in the A matrix as formulated for the Track Unknown solution (as described in section 4.2.2 (i)):

$$x = \begin{bmatrix} dX \\ dY \\ dZ \\ \Delta t \end{bmatrix}; \; A = \begin{bmatrix} l_1 & m_1 & n_1 & 1 \\ l_2 & m_2 & n_2 & 1 \\ \vdots & \vdots & \vdots & \vdots \\ l_n & m_n & n_n & 1 \\ -m_1 & 1 & 0 & 0 \\ -m_2 & 0 & 1 & 0 \end{bmatrix}.$$

When constructing C_l for this problem we have to decide which value represents the precision of the observation of the line: the precision of m or the precision of c?

On reflection it is apparent there are two observed parameters per equation (m and c). In order to solve this problem a general least squares approach must therefore be adopted.

(ii) **General Least Squares with Track Line as Observation Equations**

This technique allows us to have more than one observed parameter per equation and so allows inclusion of the two projected line equations as observations.

The least squares equations must be formulated as $Ax + Cv = b$.

A, x and C_l are as formulated for the Track Unknown solution (as described in section 4.2.2) and

$$C = \begin{bmatrix} \frac{\partial f_1}{\partial m_1} & \frac{\partial f_1}{\partial m_2} & \frac{\partial f_1}{\partial c_1} & \frac{\partial f_1}{\partial c_2} \\ \frac{\partial f_2}{\partial m_1} & \frac{\partial f_2}{\partial m_2} & \frac{\partial f_2}{\partial c_1} & \frac{\partial f_2}{\partial c_2} \end{bmatrix} = \begin{bmatrix} -X_P & 0 & -1 & 0 \\ 0 & -X_P & 0 & -1 \end{bmatrix}; \; v = \begin{bmatrix} m_1 \\ m_2 \\ c_1 \\ c_2 \end{bmatrix}$$

If Q is defined as $Q = CW^{-1}C^T$, then the solution is

$$A^T Q^{-1} Ax = A^T Q^{-1} b.$$

We can compute $C_x^{(X,Y,Z,t)} = \left(A^T Q^{-1} A\right)^{-1}$ and

$C_v = W^{-1}C^T Q^{-1}\left\{CW^{-1} - A\left[A^T Q^{-1} A\right]^{-1} A^T Q^{-1} CW^{-1}\right\}$ (Cross, 1984).

We can then proceed as described in section 4.2.2.

This method enables a position to be determined with a minimum of two visible satellites, although the solution is not necessarily located on the track. It would be possible to project the solution to the nearest point of a track database, but a simpler technique is to constrain the solution to the line of the track.

(iii) **Track as Constraint Equations**

In this method the line equations are constraints rather than observations, with the result that the solution will always lie on the track.

Since the track lines equations are not observations, it is not necessary to employ general least squares.

We have A, x and C_l the same as in the track unknown solution (see section 4.2.2) with the two equations of the projected lines as in (i) above, and want to constrain the solution to lie on both of these projected lines.

The two line equations must be expressed in the form $Ex = d$:

$$E = \begin{bmatrix} \frac{\partial f_1}{\partial X_p} & \frac{\partial f_1}{\partial Y_p} & \frac{\partial f_1}{\partial Z_p} & \frac{\partial f_1}{\partial \Delta t} \\ \frac{\partial f_2}{\partial X_p} & \frac{\partial f_2}{\partial Y_p} & \frac{\partial f_2}{\partial Z_p} & \frac{\partial f_2}{\partial \Delta t} \end{bmatrix} = \begin{bmatrix} -m_1 & 1 & 0 & 0 \\ -m_2 & 0 & 1 & 0 \end{bmatrix}; \; d = \begin{bmatrix} 0 \\ 0 \end{bmatrix}.$$

This is added as a constraint and the solution is then computed using hyper matrices as described in section 4.2.3 (iv) – (xiv), except that C_x, $C_{\hat{l}}$, C_v and the external reliability vector are the same as in section 4.2.2, N_1 is a 6×6 matrix, p_k is $n \times 1$ and p_1 is 6×1.

This technique will ensure a position which lies on the track. However, low track precision may reduce the quality of the solution because the track effectively has infinite weighting. The track precision is not factored in to the least squares adjustment, so this effect will not be quantified. Therefore overly optimistic results will be produced when using a low-precision track database.

(iv) **Track as Constraint Equations with End Points as Variables**

The technique decided upon and implemented in the spreadsheet (see section 4.2.3 for construction of matrices) is the same as (iii) above, but with the introduction of the co-ordinates of the two end points of the track, (X_1, Y_1, Z_1) and (X_2, Y_2, Z_2), as variables that can be changed as a result of the adjustment. This means that the solution is constrained to lie on the track, but the position of the track is refined by each GPS measurement made along it. Therefore low precision end points will be improved and will not reduce the precision of the solution. It is also possible that this technique could be used to collect and refine data for a track database.

2.2 SATELLITE POSITION DATA

Satellite co-ordinates were obtained from a precise ephemeris file for 21/05/05 downloaded from the National Geospatial Intelligence Agency website[1]. This file was edited with a macro-based text editor and imported into Excel, providing WGS84 co-ordinates for each satellite at 15 minute intervals throughout a 24-hour period.

2.3 USE OF ALONG-TRACK RESULTS

It is likely that the computed position would either be constrained to lie on the track or projected to the closest point on a track database. Train operators need to determine the minimum safe distance between trains and hence are only interested in positional uncertainty or detection of gross errors in the along-track direction. This is therefore the primary area of interest in our analysis.

2.4 NOTATION

(a) Superscript on a covariance matrix (C) refers to the co-ordinate system, e.g. $C_x^{(X,Y,Z,t)}$ is the covariance matrix of the parameters in the Cartesian co-ordinate system (WGS84), containing σ_X^2, σ_Y^2 and σ_Z^2 as well as the variance and covariance of any other parameters.

(b) Subscript P refers to the provisional co-ordinates of the test point: (X_p, Y_p, Z_p).

(c) Subscript 1 or 2 refers to the co-ordinates of point P_1 and point P_2 respectively, at either end of the straight line of track containing the test point: (X_1, Y_1, Z_1) and (X_2, Y_2, Z_2).

(d) The phrase "Track Precision" refers to $\sigma = \sigma_{\phi 1} = \sigma_{\lambda 1} = \sigma_{h1} = \sigma_{\phi 2} = \sigma_{\lambda 2} = \sigma_{h2}$.

(e) 'n' refers to the number of visible satellites in a given epoch.

[1] http://earth-info.nga.mil/GandG/sathtml/PEexe.html

3. SPREADSHEET OUTLINE

This chapter describes the inputs and outputs of the spreadsheet and justifies the values chosen.

3.1 INPUTS

- Latitude, longitude and height (WGS84) of two points P_1 and P_2 that define the straight line of track upon which the train currently lies: $P_1 = (\phi_1, \lambda_1, h_1)$, $P_2 = (\phi_2, \lambda_2, h_2)$.
- The precision of these points. Precisions in National Grid co-ordinates are effectively the same as in geodetic co-ordinates: $(\sigma^2_{\phi 1}, \sigma^2_{\lambda 1}, \sigma^2_{h1})$, $(\sigma^2_{\phi 2}, \sigma^2_{\lambda 2}, \sigma^2_{h2})$.
- The approximate current position P_T as a proportion of the distance along the vector from P_1 to P_2. This provides a provisional position which is required to calculate satellite visibility and to formulate constraint equations: k.
- Rotation angle about the Z-axis of the two projection planes. See section 5.1.1 for a discussion of this. In the UK, the best value is around 45°: ζ.
- Values for calculation of upper bound on Marginally Detectable Error (MDE). Percentage of good observations rejected and percentage chance of detection: α and β, respectively. See section 3.2 (a) for discussion of values chosen.
- Variance of a vertical GPS pseudo-range measurement in metres: σ_r^2.
- Satellite elevation cut-off angle – satellites are disregarded below this angle. See section 3.2 (b) for further discussion of values chosen.
- The angle from the GPS receiver to the top of the cutting on each side (ω). Although the calculations (see figure 4.1) assume the receiver lies on the bottom of a V-shaped cutting, this situation can be though of as representing the regions from where signals are blocked rather than the physical shape of the cutting. 'Right' and 'Left' are defined relative to the vector $P_1 \rightarrow P_2$: ω_{Right}, ω_{Left}.
- 'No Position' cut-off for σ_{Along} and Max δ_{Along}. If the results are greater than this then 'No Position' is returned. See section 5.1.2 for discussion of the reason for this and section 3.2 (c) for justification of values chosen.

3.2 JUSTIFICATION OF INPUT VALUES

(a) **Upper Bound on MDE: choice of α and β**

- α : The higher this value, the higher proportion of 'good' (i.e. no gross error) observations that are rejected. A standard value of 1% has been chosen.
- β : Train positioning is a safety critical application, so we need to be extremely confident of detecting gross errors of the size specified. The chosen value for this input is therefore very high, at 99.999999% (advised by Martyn Thomas of the Rail Safety and Standards Board).

(b) **Satellite Elevation Angle Cut-Off**

The usual value for survey applications is 15°, but here we are more interested in obtaining a position in the presence of obstructions rather than high precision. We therefore use the more tolerant value of 10° to increase the number of potentially visible satellites.

(c) **'No Position' Cut-Offs**

These values were advised by Martyn Thomas of the Rail Safety and Standards Board:

- $\sigma_{Along} = 10m$;
- Max $\delta_{Along} = 150m$.

(d) **Variance of a Vertical Pseudo-Range Measurement, σ_r^2**

This was taken as a standard value of $\sigma_r^2 = 1m$.

3.3 INTERMEDIATE OUTPUTS

- Azimuth of cutting: β.
- Gradient of cutting: κ.

3.4 FINAL OUTPUTS

For each epoch:

- Number of visible satellites.
- For Track Known and Track Unknown solutions:
  - Precision - along-track standard error: σ_{Along}.
  - External reliability – maximum gross error in along-track position that is undetectable with probability β (as defined in section 3.1):

    Max δ_{Along}.

4. SPREADSHEET CALCULATIONS

This chapter presents the calculations used in the spreadsheet, along with some derivations.

4.1 GENERAL CALCULATIONS

(i) **Transformation of End Points of Line from Geodetic Co-ordinates to Cartesian Co-ordinates**

If a and e are specified WGS84 parameters then for each end point we can define $\nu = \frac{a}{\left(1 - e^2 \sin^2 \phi\right)^{\frac{1}{2}}}$. Then

$X = (\nu + h)\cos\phi\cos\lambda;$

$Y = (\nu + h)\cos\phi\sin\lambda;$

$Z = \left(\left(1 - e^2\right)\nu + h\right)\sin\phi.$

(ii) **Transformation of End Point Precision from Geodetic Co-ordinates to Cartesian Co-ordinates**

Precisions entered in National Grid co-ordinates (E, N, h) are effectively the same as in geodetic co-ordinates (ϕ, λ, h), due to the small values involved.

We form $C_l^{(\mathrm{E_1N_1h_1E_2N_2h_2})} = \begin{bmatrix} \sigma_{E1}^2 & & 0 \\ & \ddots & \\ 0 & & \sigma_{h2}^2 \end{bmatrix}$, a 6x6 matrix.

Rotating this gives a full covariance matrix:

$C_l^{(\mathrm{X_1Y_1Z_1X_2Y_2Z_2})} = RC_l^{(\mathrm{E_1N_1h_1E_2N_2h_2})}R^T$, where

$$R = \begin{bmatrix} -\sin\lambda & \cos\lambda & 0 & 0 & 0 & 0 \\ -\sin\phi\cos\lambda & -\sin\phi\sin\lambda & \cos\phi & 0 & 0 & 0 \\ \cos\phi\cos\lambda & \cos\phi\sin\lambda & \sin\phi & 0 & 0 & 0 \\ 0 & 0 & 0 & -\sin\lambda & \cos\lambda & 0 \\ 0 & 0 & 0 & -\sin\phi\cos\lambda & -\sin\phi\sin\lambda & \cos\phi \\ 0 & 0 & 0 & \cos\phi\cos\lambda & \cos\phi\sin\lambda & \sin\phi \end{bmatrix}^{-1}.$$

(iii) **Calculation of Vector from P_1 to P_2**

The vector $P_1 \rightarrow P_2$ is $(X_1, Y_1, Z_1) + \lambda(\Delta X, \Delta Y, \Delta Z)$, where

$\Delta X = X_2 - X_1$, $\Delta Y = Y_2 - Y_1$ and $\Delta Z = Z_2 - Z_1$.

(iv) **Calculation of Provisional Test Point in Cartesian Co-ordinates**

We have specified k in section 3.1 as the position of the provisional point given as the proportion of the distance along $P_1 \rightarrow P_2$. The provisional point is then:

$(X_p, Y_p, Z_p) = (X_1, Y_1, Z_1) + k(\Delta X, \Delta Y, \Delta Z)$.

(v) **Transformation of Provisional Point from Cartesian Co-ordinates to Geodetic Co-ordinates**

If a, b and e are specified WGS84 parameters, we define:

$$u = \tan^{-1}\left(\frac{aZ_p}{b\left(X_p^{\,2} + Y_p^{\,2}\right)^{\frac{1}{2}}}\right);$$

$$\nu = \frac{a}{\left(1 - e^2 \sin^2 \phi_p\right)^{\frac{1}{2}}};$$

$$\varepsilon = \frac{e^2}{\left(1 - e^2\right)}.$$

Then

$$\phi_p = \tan^{-1}\left(\frac{\left(Z_p + \varepsilon b \sin^3 u\right)}{\left(\left(X_p^{\,2} + Y_p^{\,2}\right)^{\frac{1}{2}} - e^2 a \cos^3 u\right)}\right);$$

$$\lambda_p = \tan^{-1}\left(\frac{Y_p}{X_p}\right);$$

$$h_p = \frac{p}{\cos\phi_p} - \nu.$$

(vi) **Computation of Azimuth of Cutting, β**

$$\beta = \tan^{-1}\left(\frac{-\Delta X \sin\lambda_1 + \Delta Y \cos\lambda_1}{-\Delta X \sin\phi_1 \cos\lambda_1 - \Delta Y \sin\phi_1 \sin\lambda_1 + \Delta Z \sin\phi_1}\right).$$

This is the azimuth from P_1 to P_2: over short distances the azimuth from P_2 to P_1 will be effectively the same.

(vii) **Computation of Gradient of Cutting, κ**

$$\kappa = \sin^{-1}\left(\frac{h_2 - h_1}{\sqrt{\Delta X^2 + \Delta Y^2 + \Delta Z^2}}\right).$$

(viii) **Rotation of Cartesian Co-ordinates for Vector $P_1 \rightarrow P_2$ and P_T**

In order to project the vector $P_1 \rightarrow P_2$ onto the two specified planes, each element is rotated by a specified angle ξ (see section 3.1) about the Z-axis (for explanation see section 5.1.1). The provisional point P_T is also rotated.

$X' = X\cos\xi - Y\sin\xi$;

$Y' = X\sin\xi + Y\cos\xi$;

$Z' = Z$.

(ix) **Projection of Rotated Vector**

We have a rotated vector $P_1 \rightarrow P_2$: $(X_1', Y_1', Z_1') + \lambda(\Delta X', \Delta Y', \Delta Z')$.

Projection to the $X'-Y'$ plane gives the vector $(X_1', Y_1') + (\Delta X', \Delta Y')$;

Similarly , projection to the $X'-Z'$ plane gives the vector $(X_1', Z_1') + (\Delta X', \Delta Z')$.

(x) **Calculation of Gradients of Projected Lines, m_1 and m_2**

We have the vector equations of two projected lines, as shown in (ix) above.

The gradient on the $X'-Y'$ plane is $m_1 = \dfrac{\Delta Y'}{\Delta X'}$

and the gradient on the $X'-Z'$ plane is $m_2 = \dfrac{\Delta Z'}{\Delta X'}$.

(xi) **Calculation of Statistic for Upper Bound on MDE, d_i^u**

$d_i^u = a + b$, where a and b are found from the standard normal distribution tables:

a from 2-tailed test with probability α;

b from 1-tailed test with probability β.

Where α and β are defined in section 3.1 with values justified in section 3.2 (b).

4.2 CALCULATIONS FOR EACH EPOCH

4.2.1 CALCULATION OF SATELLITE VISIBILITY FOR EACH SATELLITE

(i) **Computation of Satellite Azimuth and Elevation**

The satellite co-ordinates are known in WGS84: in order to compute the azimuth and elevation they must be translated and rotated into a local topographic co-ordinate system, aligned with the National Grid with the origin at the test point.

In WGS84 the satellite co-ordinates are $\left(X_e^S, Y_e^S, Z_e^S\right)$; the co-ordinates of the test point are $\left(X_e^P, Y_e^P, Z_e^P\right)$.

Then the translated co-ordinates are:

$X_{ep}^S = X_e^S - \left(v + h_p\right)\cos\phi_p \cos\lambda_p = X_e^S - X_e^P;$

$Y_{ep}^S = Y_e^S - \left(v + h_p\right)\cos\phi_p \sin\lambda_p = Y_e^S - Y_e^P;$

$Z_{ep}^S = Z_e^S - \left(v\left(1 - e^2\right) + h_p\right)\sin\phi_p = Z_e^S - Z_e^P.$

Where v and e are as defined in 4.1 (v).

Rotating gives (in the local topographic co-ordinate system):

$X_t^S = -X_{ep}^S \sin\lambda_p + Y_{ep}^S \cos\lambda_p;$

$Y_t^S = -X_{ep}^S \sin\phi_p \cos\lambda_p - Y_{ep}^S \sin\phi_p \sin\lambda_p + Z_{ep}^S \cos\phi_p;$

$Z_t^S = X_{ep}^S \cos\phi_p \cos\lambda_p + Y_{ep}^S \cos\phi_p \sin\lambda_p + Z_{ep}^S \sin\phi_p$

Then satellite azimuth $\alpha = \tan^{-1}\left(\frac{X_t^S}{Y_t^S}\right)$

and satellite elevation $\rho = \tan^{-1}\left(\frac{Z_t^S}{\left(\left(X_t^S\right)^2 + \left(Y_t^S\right)^2\right)^{\frac{1}{2}}}\right)$.

(ii) **Calculation of Gradient Addition, υ**

This value is used to partially correct the results for a sloping track line (i.e. $h_1 \neq h_2$). See section 5.2.1 for discussion.

$\upsilon = \kappa \cos\alpha$, where κ is the gradient of the cutting (4.1 (vii)) and α is the azimuth of the satellite ((i), above). If $\upsilon < 0$ then it is set to 0 to prevent the inclusion of additional satellites, as explained in section 5.2.1.

(iii) **Computation of Bearing of Satellite from Axis of Cutting, γ**

The axis of the cutting is the line of the railway, as defined by the vector $P_1 \rightarrow P_2$. The bearing from the axis of the cutting to the satellite is $\gamma = \alpha - \beta$, where α is the azimuth of the satellite ((i)) and β is the azimuth of the cutting (4.1 (vi)).

(iv) **Testing to Determine Over which Side of the Cutting the Satellite Lies**

If $0 \leq \gamma < 180°$ then the minimum visible satellite elevation angle for the specified γ is computed using the elevation angle ω_{Right}; if $180 \leq \gamma < 360°$ then it is computed using ω_{Left}. See section 3.1 for the definition of ω_{Right} and ω_{Left}.

(v) **Computation of Minimum Visible Elevation Angle, μ'**

Figure 4.1 illustrates the derivation of the minimum elevation angle μ at which a satellite at a bearing of γ from the axis of a cutting elevation ω is visible.

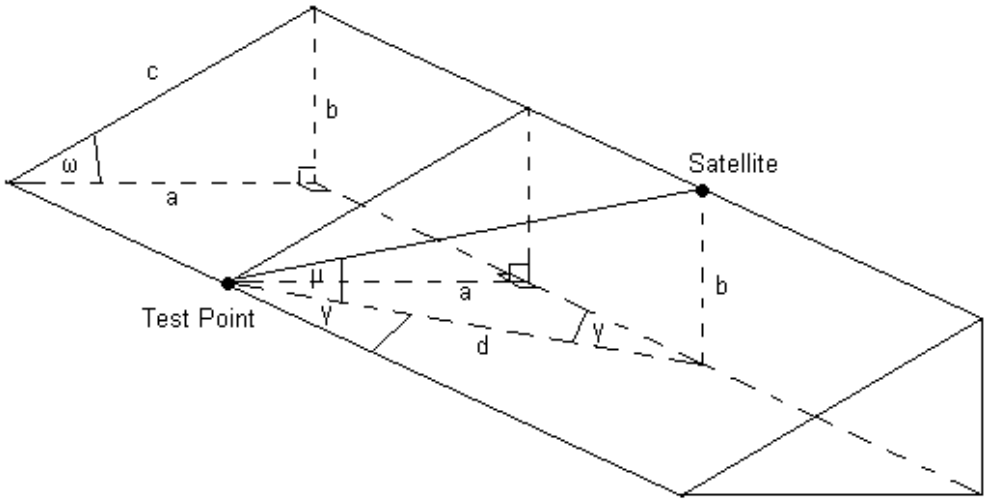

Figure 4.1: Minimum Visible Elevation Angle

From figure 4.1 we have $\tan\omega = \frac{b}{a}$.

Since the scale is arbitrary we can assume $a = 1$, so $\tan\omega = b$.

We can then compute $d = \frac{a}{\sin\gamma} = \frac{1}{\sin\gamma}$ (γ is computed in (iii) above).

From this we can calculate $\cos\mu = \frac{d}{\sqrt{b^2 + d^2}}$, and so $\mu = \cos^{-1}\left(\frac{d}{\sqrt{b^2 + d^2}}\right)$.

The gradient addition is then added to give $\mu' = \mu + \upsilon$.

(vi) **Determination of Satellite Visibility**

A given satellite is visible if $\rho \geq \mu'$, i.e. its elevation is greater than minimum visible elevation angle calculated for that satellite in (v) above. .

4.2.2 CALCULATION OF TRACK UNKNOWN SOLUTION

(i) **Formation of Design Matrix,** A

The linearised observation equations for n satellites give us

$$A = \begin{bmatrix} l_1 & m_1 & n_1 & 1 \\ l_2 & m_2 & n_2 & 1 \\ \vdots & \vdots & \vdots & \vdots \\ l_n & m_n & n_n & 1 \end{bmatrix}; \; x = \begin{bmatrix} dX_p \\ dY_p \\ dZ_p \\ \Delta t_p \end{bmatrix}.$$

If the co-ordinates of satellite i are $\left(X^i, Y^i, Z^i\right)$ and the co-ordinates of the test point are $\left(X_p, Y_p, Z_p\right)$ then

$$l_i = \frac{X_p - X^i}{\left(\left(X^i - X_p\right)^2 + \left(Y^i - Y_p\right)^2 + \left(Z^i - Z_p\right)^2\right)^{\frac{1}{2}}};$$

$$m_i = \frac{Y_p - Y^i}{\left(\left(X^i - X_p\right)^2 + \left(Y^i - Y_p\right)^2 + \left(Z^i - Z_p\right)^2\right)^{\frac{1}{2}}};$$

$$n_i = \frac{Z_p - Z^i}{\left(\left(X^i - X_p\right)^2 + \left(Y^i - Y_p\right)^2 + \left(Z^i - Z_p\right)^2\right)^{\frac{1}{2}}}.$$

(ii) **Formation of Covariance Matrix of the Observations,** C_l

We have $C_l = \begin{bmatrix} f(\rho_1) & 0 & \dots & 0 \\ 0 & f(\rho_2) & \cdots & 0 \\ \vdots & \vdots & \ddots & \vdots \\ 0 & 0 & \dots & f(\rho_n) \end{bmatrix}.$

If σ_v^2 is the specified variance of a vertical pseudo-range measurement (section 3.1) and ρ_i is the elevation angle of satellite i (section 4.2.1 (i)), then

$$f(\rho_i) = \frac{\sigma_v^2}{\sin^2 \rho_i}.$$

We can then compute the weight matrix $W = C_l^{-1}$.

(iii) **Calculation of Covariance Matrix of the Parameters,** $C_x^{(X,Y,Z,t)}$

$C_x^{(X,Y,Z,t)} = \left(A^T W A\right)^{-1}$, a 4x4 matrix.

(iv) **Rotation of $C_x^{(X,Y,Z,t)}$ to $C_x^{(E,N,h,t)}$**

In order to obtain along-track results, the covariance matrix of the parameters is initially rotated to the local topographic co-ordinate system.

$C_x^{(E,N,h,t)} = RC_x^{(X,Y,Z,t)}R^T$, where

$$R = \begin{bmatrix} -\sin\lambda_p & \cos\lambda_p & 0 & 0 \\ -\sin\phi_p\cos\lambda_p & -\sin\phi_p\sin\lambda_p & \cos\phi_p & 0 \\ \cos\phi_p\cos\lambda_p & \cos\phi_p\sin\lambda_p & \sin\phi_p & 0 \\ 0 & 0 & 0 & 1 \end{bmatrix}.$$

(v) **Rotation of $C_x^{(E,N,h,t)}$ to $C_x^{(Across,Along,h,t)}$**

$C_x^{(E,N,h,t)}$ is rotated to align with the track direction to provide along-track results.

$C_x^{(Across,Along,h,t)} = R'C_x^{(E,N,h,t)}R'^T$, where

$$R' = \begin{bmatrix} \cos\beta & \sin\beta & 0 & 0 \\ -\sin\beta & \cos\beta & 0 & 0 \\ 0 & 0 & 1 & 0 \\ 0 & 0 & 0 & 1 \end{bmatrix}.$$

β is the azimuth of the cutting as computed in section 4.1 (vi).

(vi) **Calculation of Covariance Matrix of the Observed Parameters, $C_{\hat{l}}$**

$C_{\hat{l}} = AC_x^{(X,Y,Z,t)}A^T$, an $n \times n$ matrix (where n is the number of visible satellites).

(vii) **Calculation of Covariance Matrix of the Residuals, C_v**

$$C_v = C_l - C_{\hat{l}} = \begin{bmatrix} \sigma_{v1}^2 & & & \\ & \sigma_{v1}^2 & & \cdots \\ \cdots & & \ddots & \\ & & & \sigma_{vn}^2 \end{bmatrix}, \text{an } n \times n \text{ matrix.}$$

(viii) **Calculation of Upper Bound on MDE for each Observation, Δ_i^u**

If $\tau_i = \dfrac{\sigma_i}{\sigma_{vi}}$, then the upper limit on Marginally Detectable Error for the ith observation is $\Delta_i^u = d_i^u\tau_i\sigma_i$, where d_i^u is calculated as in section 4.1 (xi).

(ix) **Calculation of External Reliability (X,Y,Z)**

To calculate the effect on the solution of the maximum gross error undetectable with specified probability (see section 3.1) in the k[th] observation, we form

$p_k = \begin{bmatrix} 0 \\ \vdots \\ \Delta_k^u \\ \vdots \\ 0 \end{bmatrix}$. We then evaluate $\left(A^T W A\right)^{-1} A^T W p_k = \begin{bmatrix} \delta X \\ \delta Y \\ \delta Z \\ \delta t \end{bmatrix}$.

where δ represents the effect of the largest undetectable error on that variable. This process is carried out for $k = 1...n$.

(x) **Rotation of External Reliability Vector to (E,N,h)**

In order to obtain along-track results, the external reliability vector is initially rotated to the local topographic co-ordinate system.

$\delta_E = -\delta_X \sin\lambda_p + \delta_Y \cos\lambda_p$;

$\delta_N = -\delta_X \sin\phi_p \cos\lambda_p - \delta_Y \sin\phi_p \sin\lambda_p + \delta_Z \cos\phi_p$;

$\delta_h = \delta_X \cos\phi_p \cos\lambda_p + \delta_Y \cos\phi_p \sin\lambda_p + \delta_Z \sin\phi_p$.

ϕ_p is the latitude and λ_p is the longitude of the provisional point (4.1 (v)).

(xi) **Rotation of External Reliability Vector to (Across,Along,h)**

The external reliability vector is then rotated to align with the track direction to provide along-track results.

$\delta_{Along} = \delta_E \sin\beta + \delta_N \cos\beta$;

$\delta_{Across} = \delta_E \cos\beta + \delta_N \sin\beta$.

β is the azimuth of the cutting as computed in4.1 (vi).

The maximum δ_{Along} of all observations for a given epoch represents the maximum possible error in position that is undetectable with the specified probability (section 3.1).

4.2.3 CALCULATION OF TRACK KNOWN SOLUTION

(i) **Formation of Design Matrix,** A

See section 2.1.2 for discussion of methods for incorporating knowledge of the track into the least squares adjustment.

$$A = \begin{bmatrix} & & & & 1 & 0 & 0 & 0 & 0 & 0 \\ & & & & 0 & 1 & 0 & 0 & 0 & 0 \\ & & & & 0 & 0 & 1 & 0 & 0 & 0 \\ & 0 & & & 0 & 0 & 0 & 1 & 0 & 0 \\ & & & & 0 & 0 & 0 & 0 & 1 & 0 \\ & & & & 0 & 0 & 0 & 0 & 0 & 1 \\ l_1 & m_1 & n_1 & 1 & & & & & & \\ l_2 & m_2 & n_2 & 1 & & & 0 & & & \\ \vdots & \vdots & \vdots & \vdots & & & & & & \\ l_n & m_n & n_n & 1 & & & & & & \end{bmatrix}; \; x = \begin{bmatrix} dX_p \\ dY_p \\ dZ_p \\ \Delta t \\ dX_1 \\ dY_1 \\ dZ_1 \\ dX_2 \\ dY_2 \\ dZ_2 \end{bmatrix},$$

where $l_i = \dfrac{X_p - X^i}{\left(\left(X^i - X_p\right)^2 + \left(Y^i - Y_p\right)^2 + \left(Z^i - Z_p\right)^2\right)^{\frac{1}{2}}}$;

$m_i = \dfrac{Y_p - Y^i}{\left(\left(X^i - X_p\right)^2 + \left(Y^i - Y_p\right)^2 + \left(Z^i - Z_p\right)^2\right)^{\frac{1}{2}}}$;

$n_i = \dfrac{Z_p - Z^i}{\left(\left(X^i - X_p\right)^2 + \left(Y^i - Y_p\right)^2 + \left(Z^i - Z_p\right)^2\right)^{\frac{1}{2}}}$ as before (see section 4.2.2 (i))

Here x is a 10×1 matrix and A is a $(n+6) \times 10$ matrix.

(ii) **Formation of Constraint Equations**

We have two constraint equations corresponding to the projection of the line to each plane:

$$f_1\left(X_p, Y_p, Z_p, \Delta t, X_1, Y_1, Z_1, X_2, Y_2, Z_2\right) = Y_P - m_1 X_p - c_1,$$

$$f_2\left(X_p, Y_p, Z_p, \Delta t, X_1, Y_1, Z_1, X_2, Y_2, Z_2\right) = Z_P - m_2 X_p - c_2,$$

where $m_1 = \dfrac{Y_2 - Y_1}{X_2 - X_1}$, $m_2 = \dfrac{Z_2 - Z_1}{X_2 - X_1}$,

and $c_1 = Y_1 - m_1 X_1$, $c_2 = Z_1 - m_2 X_1$.

These need to be expressed in the form $Ex = d$, with x as in (i) above.

Linearisation gives both equations as:

$$\begin{bmatrix} \frac{\partial f_1}{\partial X_p} & \frac{\partial f_1}{\partial Y_p} & \frac{\partial f_1}{\partial Z_p} & \frac{\partial f_1}{\partial t} & \frac{\partial f_1}{\partial X_1} & \frac{\partial f_1}{\partial Y_1} & \frac{\partial f_1}{\partial Z_1} & \frac{\partial f_1}{\partial X_2} & \frac{\partial f_1}{\partial Y_2} & \frac{\partial f_1}{\partial Z_2} \\ \frac{\partial f_2}{\partial X_p} & \frac{\partial f_2}{\partial Y_p} & \frac{\partial f_2}{\partial Z_p} & \frac{\partial f_2}{\partial t} & \frac{\partial f_2}{\partial X_1} & \frac{\partial f_2}{\partial Y_1} & \frac{\partial f_2}{\partial Z_1} & \frac{\partial f_2}{\partial X_2} & \frac{\partial f_2}{\partial Y_2} & \frac{\partial f_2}{\partial Z_2} \end{bmatrix} x = \begin{bmatrix} 0 \\ 0 \end{bmatrix}$$

$$\begin{bmatrix} -m_1 & 1 & 0 & 0 & \frac{m_1}{\Delta X}\left(X_p + X_1 + \frac{1}{\Delta X}\right) & \frac{1}{\Delta X}\left(X_p - X_2\right) & 0 & \frac{m_1}{\Delta X}\left(X_p - X_1\right) & \frac{1}{\Delta X}\left(X_1 - X_p\right) & 0 \\ -m_2 & 0 & 1 & 0 & \frac{m_2}{\Delta X}\left(X_p + X_1 + \frac{1}{\Delta X}\right) & 0 & \frac{1}{\Delta X}\left(X_p - X_2\right) & \frac{m_2}{\Delta X}\left(X_p - X_1\right) & 0 & \frac{1}{\Delta X}\left(X_1 - X_p\right) \end{bmatrix} x = \begin{bmatrix} 0 \\ 0 \end{bmatrix}$$

where $\Delta X = X_2 - X_1$.

(iii) **Formation of Covariance Matrix of the Observations,** C_l

$$C_l = \begin{bmatrix} \left[C_l^{(X_1 Y_1 Z_1 X_2 Y_2 Z_2)}\right] & [0] \\ [0] & \begin{bmatrix} f(\rho_1) & 0 & \cdots & 0 \\ 0 & f(\rho_2) & \cdots & 0 \\ \vdots & \vdots & \ddots & \vdots \\ 0 & 0 & \cdots & f(\rho_n) \end{bmatrix} \end{bmatrix}$$

where $C_l^{(X_1 Y_1 Z_1 X_2 Y_2 Z_2)}$ is the full covariance matrix of the precisions of the end points of the line as calculated in section 4.1 (ii), σ_v^2 is the specified variance of a vertical pseudo-range measurement (section 3.1), ρ_i is the elevation angle of satellite i (section 4.2.1 (i)) and $f(\rho_i) = \dfrac{\sigma_v^2}{\sin^2 \rho_i}$.

We can then compute the weight matrix $W = C_l^{-1}$.

Both W and C_l have dimension $(n+6)\times(n+6)$.

(iv) **Formation of Hyper Matrix,** N_1

The constraints are applied to make a 12×12 hyper matrix:

$$N_1 = \begin{bmatrix} A^T W A & E^T \\ E & 0 \end{bmatrix}.$$

(v) **Calculation of Covariance Matrix of the Parameters,** $C_x^{(X,Y,Z,t)}$

$N_1^{-1} = \begin{bmatrix} C_x^{(X,Y,Z,t)} & [10\times 2] \\ [2\times 10] & [2\times 2] \end{bmatrix}$, a 12×12 matrix.

That is $C_x^{(X,Y,Z,t)}$ comprises the top left 10×10 elements of N_1^{-1} (Leick, 2004).

(vi) **Rotation of** $C_x^{(X,Y,Z,t)}$ **to** $C_x^{(E,N,h,t)}$

In order to obtain along-track results, the covariance matrix of the parameters is initially rotated to the local topographic co-ordinate system.

The rotation only applies to X_p, Y_p, Z_p and t, the top left 4x4 matrix of $C_x^{(X,Y,Z,t)}$. This is because the other entries in $C_x^{(E,N,h,t)}$ for the Track Known solution are variances and covariances of the line end points P_1 and P_2, and we are not interested in the precision of these in the along-track direction. This rotation is the same as section 4.2.2 (iv).

(vii) **Rotation of** $C_x^{(E,N,h,t)}$ **to** $C_x^{(Across,Along,h,t)}$

This rotation is the same as section 4.2.2 (v).

(viii) **Calculation of Covariance Matrix of the Observed Parameters,** $C_{\hat{l}}$

This is the same as section 4.2.2 (vi), except it results in an $(n+6)\times(n+6)$ matrix.

(ix) **Calculation of Covariance Matrix of the Residuals,** C_v

This is the same as section 4.2.2 (vii), except it results in an $(n+6)\times(n+6)$ matrix.

(x) **Calculation of Upper Bound on MDE for each Observation,** Δ_i^u

This is the same as section 4.2.2 (viii), except there are 6 additional observations.

(xi) **Formation of Hyper Matrix For External Reliability Calculation,** p_{1k}

For each observation, we form $p_k = \begin{bmatrix} 0 \\ \vdots \\ \Delta_k^u \\ \vdots \\ 0 \end{bmatrix}$, a $(n+6)\times 1$ vector. Then we can calculate $p_{1k} = \begin{bmatrix} A^T W p_k \\ 0 \\ 0 \end{bmatrix}$.

(xii) **Calculation of External Reliability (X,Y,Z)**

To calculate the effect on the solution of the maximum error undetectable with specified probability (section 3.1) in the kth observation, we evaluate:

$$(N_1)^{-1} p_{1k} = \begin{bmatrix} \delta X_p \\ \delta Y_p \\ \delta Z_p \\ \delta t \\ \delta X_1 \\ \delta Y_1 \\ \delta Z_1 \\ \delta X_2 \\ \delta T_2 \\ \delta Z_2 \end{bmatrix},$$

where δ represents the effect of the largest undetectable error.

This process is carried out for $k = 1..(n+6)$.

(xiii) **Rotation of External Reliability Vector to (E,N,h)**

This is the same as section 4.2.2 (x).

(xiv) **Rotation of External Reliability Vector to (Across,Along,h)**

This is the same as section 4.2.2 (xi).

5. SPREADSHEET PROBLEMS

This chapter discusses the problems encountered during the construction of the spreadsheet. Section 5.1 covers those which have been solved, whilst section 5.2 covers problems where the solution lies beyond the scope of this project.

5.1 SOLVED PROBLEMS

5.1.1 ERRORS IN EXTERNAL RELIABILITY CALCULATIONS FOR TRACK KNOWN SOLUTION

For cutting azimuths close to 90° or 270°, high (>60°) cutting side angles and few visible satellites (3-4), it was observed that the variances of the residuals for Y_1, X_2 and Y_2 were often small (<10^{-10}m) and negative. This occurred irrespective of which two planes the track line was projected to (from X-Y, X-Z and Y-Z). These values should never be negative as this implies $\sigma_l^2 < \sigma_{\hat{l}}^2$, i.e. we know the parameter worse after least squares adjustment than before. It is therefore likely that these values result from small calculation errors made by Excel. Numbers stored on a computer have finite length and hence precision, so dividing by very small numbers can create a very large and inaccurate number. This is a particular problem in matrix multiplication or inversion, both of which are used extensively in the spreadsheet. Analysis of such problems is beyond the scope of this project, a geometrical consideration of the situation is given below.

The test points all lie within the UK. Since the X-axis of WGS84 passes through Greenwich, the test lines are all very close to this axis: with azimuths of 90° or 270° they are parallel to the X-Y plane. Errors in the Y co-ordinate of either end point will have no significant effect on the gradient of the projection to any plane. If we look at the constraint equations (section 4.2.3 (ii)) we can see that the Y co-ordinate of each end point does not feature directly, but rather is included through the gradient. Therefore large errors in the measurement of these co-ordinates would not significantly change the values entered into the least squares adjustment, effectively making error detection on these measurements impossible.

This theory was corroborated by increasing the longitude of the test points by 45°, which caused the errors to disappear.

It was therefore decided to project the lines to two different planes, $X' - Y'$ and $X' - Z'$, where the X', Y', Z' co-ordinate system differs from WGS84 by a rotation of ζ about the Z-axis (see figure 5.1). This angle is chosen to keep the track line in the middle of the X' and Y' axes – in the UK a value around 45° is suitable and is one of the spreadsheet inputs described in section 3.1.

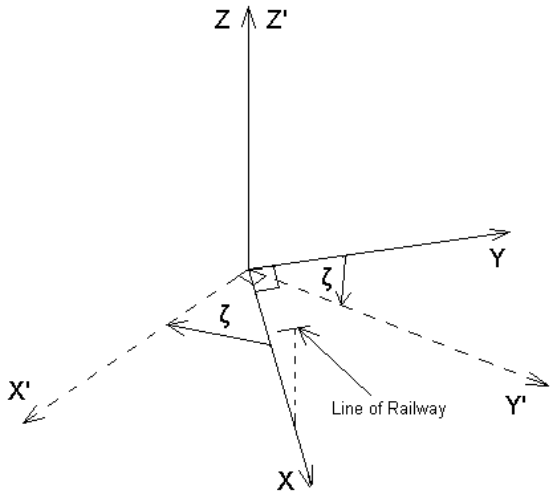

Figure 5.1: Rotation of Axes by ζ

5.1.2 Comparison Graphs Unintuitive: Introduction of "No Position" Cut-Off Parameters

When preparing a comparison between Track Known σ_{Along} and Track Unknown σ_{Along} across a range of cutting side angles it was noted that the results were unintuitive. Averaging σ_{Along} over 24 hours and 180° of cutting azimuths produced a graph as shown in figure 5.2.

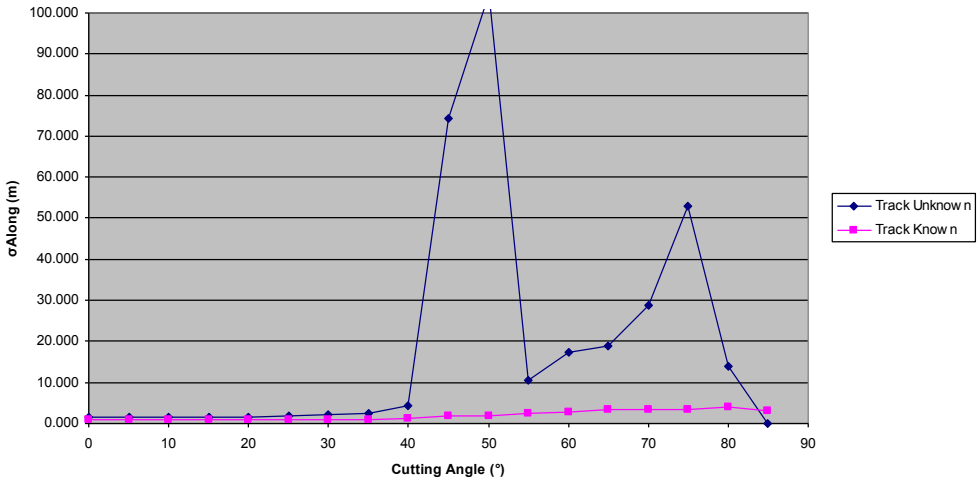

Figure 5.2: Graph of σ_{Along} Averaged over Time and Cutting Azimuth against Cutting Angle

It seems unlikely that increasing the cutting angle (and hence obscuring satellites) would increase the mean precision of position so significantly, so there must be a problem with our averaging technique.

After investigation it was discovered that for some epochs with four visible satellites (the minimum for a Track Unknown solution), σ_{Along} was very high (in some cases >20 km). It is likely that this is due to poor satellite geometry for that epoch which has less effect on the Track Known solution due to the inclusion of two additional equations.

It is clear that a position with $\sigma_{Along} = 20km$ is not useful, so a parameter was introduced to specify the maximum allowable σ_{Along}. Above this value "No Position" is returned.

The same problem was encountered and solution implemented for Max δ_{Along}. The values of these parameters were set at 10m for σ_{Along} and 150m for Max δ_{Along}, as described in section 3.2 (c).

5.2 UNSOLVED PROBLEMS

5.2.1 CALCULATIONS ASSUME HORIZONTAL CUTTING

The method for determining the minimum visible elevation angle for a satellite of given bearing from the line of the cutting (section 4.2.1 (v)) is only accurate with the initial value μ for horizontal cuttings, i.e. where each end point has the same height. In an attempt to address this problem, the gradient correction κ (calculated in section 4.2.1 (ii)) was introduced to enable satellites obscured in the up-hill direction to be disregarded. In order to determine which additional satellites are made visible in the down-hill direction it is necessary to know the distance from the current location to the bottom of the hill, as well as the terrain behind. This is beyond the scope of this spreadsheet so the current implementation only reduces the number of visible satellites, giving pessimistic results in such a situation.

5.2.2 ERRORS WHEN PRECISION OF ENDPOINTS IS LOW RELATIVE TO LINE LENGTH

It was noted that errors occurred in the spreadsheet when the precision of the endpoints was low relative to the length of the track line they defined. These errors are caused by small negative residual variances, similar to those in section 5.1.2. In this situation the magnitude of the errors is much greater ($\sim 10^{-1}$m) and the variances of the residuals of the pseudo-range measurements are affected instead. The problem occurs for all slope sides when the standard error of position of the end points is similar to the distance between them. Increasing this distance removes these errors.

Such a situation is unlikely to occur in reality – the standard error of position may be 1m or less, whereas the track sections will be tens of metres or more. Therefore this is not a problem in practice. A negative residual variance checking procedure was implemented to cause 'No Position' to be returned rather than an error for these situations.

6. SPREADSHEET VALIDATION

This chapter presents the results of validation tests made on spreadsheet.

6.1 COMPARISON WITH LEICA SATELLITE AVAILABILITY PROGRAM

To test the accuracy of the satellite visibility portion of the spreadsheet, the number of visible satellites for each epoch was compared to that predicted by Leica's Satellite Availability program.

Four comparisons were made, for cutting side angles of 10°, 30°, 50° and 70° with the following parameters:

- Cutting azimuth $\alpha = 0°$;
- Slope of cutting: $\omega_{Left} = \omega_{Right}$;
- Test point: φ = 052° 00' North, λ = 000° 07' West, h = 90m;
- All other parameters were as specified in section 3.

The number of visible satellites for each method was compared for each epoch throughout 24-hours. Due to different epoch intervals in the spreadsheet and the Satellite Availability program, the epoch interval for these comparisons was 30 minutes.

The cutting was simulated in the Satellite Availability program by the addition of visibility obstructions. This feature requires an obstruction elevation to be entered every 10° of azimuth – these values were calculated for each cutting angle using the technique described in section 4.2.1 (v). See Appendix A.1 for a listing of the azimuth and elevation point inputs for the obstruction file.

See Appendix A.2 for the results of this comparison and A.3 – A.6 for graphs of each cutting angle.

The two methods of satellite visibility determination agree closely, in general having less than one satellite difference and following the same trends over time.

A detailed analysis was made of the visible satellites in the first epoch with cutting angle 10°. Figure 6.1 shows the satellites and their corresponding azimuth and elevation angles:

Satellite PRN	Spreadsheet			Leica		
	Visible?	Azimuth α (°)	Elevation ρ (°)	Visible?	Azimuth α (°)	Elevation ρ (°)
1	Yes	300	34	Yes	301	34
2	Yes	89	27	Yes	94	28
4	Yes	41	17	Yes	45	19
5	Yes	83	53	Yes	83	58
6	Yes	197	43	Yes	200	39
9	Yes	137	21	Yes	138	24
14	Yes	247	41	Yes	249	41
20	No	342	4	Yes	345	5
25	Yes	305	27	Yes	305	29
30	Yes	280	81	Yes	276	78

Figure 6.1: Comparison of Visible Satellites at 00:00 with Cutting Angle 10°

Note that satellite PRN 20 lies below the satellite elevation cut-off for the spreadsheet (10°). Other than this difference, the same satellites are visible in both methods with almost the same azimuth and elevation. This indicates that the similar number of visible satellites is not coincidental and supports the accuracy of the spreadsheet.

6.2 COMPARISON WITH COLLECTED DATA

Satellite visibility data was collected in Cleveland Street, London for four epochs at 15 minute intervals. The street chosen is straight, level and treeless with buildings of relatively uniform height on both sides in order to simulate as closely as possible the assumptions made in the spreadsheet.

The test position was obtained from the GPS data. The elevation of each 'cutting' side was determined using a total station in the same location as the GPS receiver. The azimuth of the 'cutting' was determined using a compass on the ground and by measurement on a street map.

A comparison between the collected data and the spreadsheet was made of the satellites visible at each epoch. The spreadsheet used the following inputs:

- φ = 051° 31' 22" North, λ = 000° 8' 30" West, h = 86.841m;
- Date: 24/08/2005 (new ephemeris file used);
- $\omega_{Left} = 74°$;
- $\omega_{Right} = 46°$;
- Obstructions in the along-track directions all below the 15° cut-off;
- Azimuth of cutting $\beta = 320°$.
- All other parameters were as specified in section 3.

The results of this comparison are given in figure 6.2.

Time	Satellite	Experiment				Spreadsheet			
Epoch	PRN	L1	L2	Azimuth α (°)	Elevation ρ (°)	Visible?	Azimuth α (°)	Elevation ρ (°)	Min. Vis. Elev (°)
14:00	9	TR	TR	280	64	0	280	64	66
	18	TR	TR	266	36	0	267	37	70
	26	TR	TR	150	49	1	150	50	31
	29	TR	TR	148	37	1	148	38	25
14:15	7	TR	TR	81	35	0	82	36	41
	9	TR	TR	287	71	1	286	71	63
	26	TR	TR	152	41	1	152	43	36
	29	TR	TR	150	29	1	150	31	31
14:30	5	TR	TR	222	38	0	223	38	74
	9	TR	TR	296	77	1	295	77	56
	26	TR	TR	154	35	0	154	36	40
14:45	7	TR	SH	66	34	0	67	35	45
	9	TR	TR	317	84	1	317	84	11
	26	TR	SH	155	28	0	156	29	43

Figure 6.2: Comparison of Visible Satellites over Four Epochs

There is a considerable difference in the number of visible satellites although the azimuth and elevation of each satellite is similar in both methods. Analysis of the spreadsheet shows that many of the satellites are a few degrees below the minimum visible elevation angle, as calculated in section 4.2.1 (v). It is possible that the signals have been diffracted, but given the number of satellites affected it is more likely that this indicates a failure of the spreadsheet to model the obstructions adequately. The 'cutting' sides are assumed completely uniform, whereas in reality even a carefully chosen site such as this has enough variation to significantly alter the obtained results.

Several satellites, in particular PRN 18 at 14:00 and PRN 5 at 14:30 were visible to the receiver even though they were far below the minimum visible elevation angle, as calculated in the spreadsheet. This may indicate a greater deviation of the assumed model from reality in these directions, or the signals might be received after reflection or diffraction.

This experiment shows that the spreadsheet is inadequate for the accurate modelling of satellite visibility in a given cutting. If this was required then a detailed model of the cutting sides would have to be used. However this does not mean that the spreadsheet is useless, since we can still obtain general results that will be useful in determining the benefits of the Track Known solution.

7. ANALYSIS

This chapter utilises the completed spreadsheet to compare Track Unknown and Track Known solutions with the aim of determining the benefit derived from incorporating track knowledge in the positioning solution.

7.1 ACHIEVING A USEFUL COMPARISON

The initial step in quantifying the improvement gained using the Track Known solution is to determine which values are good indicators of quality or quality improvement.

After some initial analysis, it was ascertained that comparing the mean over all epochs of σ_{Along} or Max δ_{Along} is a poor indicator of improvement. There were often epochs where only the Track Known solution had a position with high values that biased the mean. This resulted in some comparisons showing that the Track Known solution was worse than Track Unknown: this is impossible since the Track Known solution adds information to the least squares adjustment so it should be at least as good. A more representative statistic is the mean across all epochs of the improvement in σ_{Along} or Max δ_{Along}.

Our main interest is obtaining a position, rather than precision or reliability per se. The conditions of this are:

- At least 5 (Track Unknown) or 3 (Track Known) visible satellites (required for error detection);
- σ_{Along} and Max δ_{Along} do not exceed the specified cut-off limits.

Within these conditions, improvements in precision or reliability are not especially useful. Therefore, when comparing the improvement from Track Unknown to Track Known, the most useful statistic is the additional proportion of epochs where a position satisfying the above criteria is possible, i.e. the proportion of epochs where a position is only possible with the Track Known solution.

In subsequent analyses we look at the following statistics (where appropriate):

- Number of visible satellites;
- Proportion of epochs with error detection;
- Improvement in σ_{Along}, Max δ_{Along} and proportion of epochs with error detection, both as absolute values and a percentage improvement over the Track Unknown solution.

7.2 ANALYSIS

This section consists of a series of analyses with the ultimate aim of providing a general idea about the improvement in positioning gained when using the Track Known solution in various situations.

7.2.1 ANALYSIS OF THE EFFECT OF CUTTING AZIMUTH

It is necessary to determine if the azimuth of the cutting has a significant impact on the results obtained. If it does, then in order to apply the results of further analysis to the general case we will need to average over cutting azimuth. If not then a single azimuth can be used.

The mean over 24-hours of each statistic was computed for every 10° of cutting azimuth (β). Due to the symmetry of the cutting we need only test for $0 \le \beta < 180°$.

The spreadsheet input variables were:

- Precision of track: $\sigma = 1m$;
- Slope of cutting: $\omega_{Left} = \omega_{Right} = 45°$;
- Test point: φ = 054° 08’ 00” North, λ = 003° 49’ 30” West, h = 100m;
- All other parameters were as specified in section 3.

See Appendix B.1 for a table of the results and B.2 – B.5 for graphs of the improvement in each statistic against cutting azimuth.

There is a significant variation in the results obtained for different cutting azimuths, not least the mean number of visible satellites. The graphs B.2 – B.5 show that the mean Track Known improvement over 24-hours varies significantly with cutting azimuth. For example, the improvement in the proportion of epochs where it is possible to obtain a position ranges from 22.9% with a 130° cutting azimuth to 106.7% with a 10° cutting azimuth. This significant difference means that subsequent comparisons need to be averaged over azimuth in order to draw general conclusions.

7.2.2 Analysis of the Effect of Location

We need to determine if the location of the cutting within Britain is significant for the results obtained. If there is significant variation with location then we will have to look at several points around the country in order to determine a general conclusion about the value of the Track Known solution. If they do not, we can make all subsequent analysis at a location in the centre of the country and apply the conclusions generally.

A comparison was made between two extreme points on the railway network:
SW – Penzance: φ = 051° 07' 00" North, λ = 005° 33' 00" West, h = 100m;
NE – Aberdeen: φ = 057° 09' 00" North, λ = 002° 06' 00" West, h = 100m.

This analysis has two components. The first involves a comparison of the number of visible satellites, the precision and the reliability in each location for each epoch over 24 hours, with the aim of determining how different the GPS positioning conditions are at each location.

For this comparison, we are interested in the potential difference in satellite positioning at each location irrespective of the existence of a cutting. Therefore we can set the slope sides to 0°, ignore the Track Known solution and compare the Track Unknown statistics $\sigma_{Position} = \sqrt{\sigma^2_{Along} + \sigma^2_{Across}}$ and $\delta_{Position} = \sqrt{\delta^2_{Along} + \delta^2_{Across}}$.
This means that the direction of the track has no effect, but we can compare results for each epoch directly and avoid any potential distortion from averaging over cutting azimuth. The spreadsheet therefore had the following input variables:

- Slope of cutting: $\omega_{Left} = \omega_{Right} = 0°$;
- All other parameters were as specified in section 3.

Note that since there are no obstructions to visibility, error detection is possible for all epochs.

See Appendix C.1 for a table of results and C.3 – C.5 for graphs of satellite visibility, $\sigma_{Position}$ and Max $\delta_{Position}$ for each location against time.

There is some variation between the two locations, although they follow a similar pattern. However, we can see from table C.1 and that the difference when averaged over all epochs is fairly small, e.g. 8.1 visible satellites in Penzance and 8.5 in Aberdeen.

The second comparison was made with a 45° cutting slope, averaged over time and azimuth. The aim of this was to determine the effect of location on the improvement gained with the Track Known solution.

The spreadsheet inputs were:

- Slope of cutting: $\omega_{Left} = \omega_{Right} = 45°$;
- All other parameters were as specified in section 3.

Table C.2 displays these averaged results and shows that although there is some variation with location this is fairly small, e.g. 67.9% improvement in the proportion of epochs with error detection in Penzance compared to 80.7% in Aberdeen.

In subsequent sections we will therefore draw generalised conclusions from analysis of a single location, the mean of these two positions:
φ = 054° 08’ 00” North, λ = 003° 49’ 30” West, h = 100m;

When this result is combined with section 7.2.1, we can infer that in general cuttings in the East-West direction are better for positioning than those in the North-South direction (see table B.1 and graph B.2).

7.2.3 Analysis of the Effect of Track Precision

We are now in a position to determine how the precision of the track database affects the Track Known solution. The improvement in each statistic, averaged over azimuth and 24 hours, was calculated for a range of different track precisions. For the purpose of this analysis, "Track Precision" refers to $\sigma = \sigma_{\phi 1} = \sigma_{\lambda 1} = \sigma_{h1} = \sigma_{\phi 2} = \sigma_{\lambda 2} = \sigma_{h2}$.

The spreadsheet inputs were :

- Slope of cutting: $\omega_{Left} = \omega_{Right} = 45°$;
- Test point: φ = 054° 08' 00" North, λ = 003° 49' 30" West, h = 100m;
- Mean taken over azimuth (every 15°);
- All other parameters were as specified in section 3.

See Appendix D.1 for a table of results and D.2 – D.4 for graphs showing how the improvement in each statistic changes with track precision.

We can see from these results that the improvement gained from the Track Known solution is reduced with lower end-point precision, until with $\sigma = 100m$ the benefit is minor (we can only position in an extra 1.7% of epochs). Table D.1 shows that a very precise track database brings little benefit: for $\sigma = 0.001m$ the mean improvement in the proportion of epochs with error detection is 66.9%, whereas for $\sigma = 1m$ it is 66.3%. Even with $\sigma = 5m$ we have a 62.5% improvement and at this level of precision it may be possible to obtain track data from digital maps, which would be much cheaper than surveying the whole railway network.

7.2.4 Analysis of the Effect of Cutting Side Angle

The final analysis aims to determine the effect of the steepness of the cutting sides on the usefulness of the Track Known solution. The improvement in each statistic, averaged over azimuth and 24 hours, was calculated for a range of different cutting side angles. Since the results were averaged over azimuth we keep $\omega_{Left} = \omega_{Right}$ for ease of comparison.

The spreadsheet inputs were:

- Precision of track: $\sigma = 1m$;

- Test point: φ = 054° 08’ 00” North, λ = 003° 49’ 30” West, h = 100m;
- Mean taken over azimuth (every 15°);
- All other parameters were as specified in section 3.

See Appendix E.1 for a table of results and E.2 – E.5 for graphs showing how the improvement in each statistic changes with cutting side angle.

Graph E.2 indicates that there is a linear relationship between the angle of the cutting sides and the number of visible satellites.

We can see from table E.1 and graphs E.3 – E.5 that the Track Known solution provides a greater percentage improvement as the cutting side angle increases. This means that the Track Known solution is relatively more useful in steeper cuttings. This is intuitive since steeper cuttings mean fewer visible satellites, which makes the two track equations relatively more important for the quality of the solution, or for obtaining a solution at all.

7.3 CONCLUSION – ANALYSIS OF THE EFFECTIVENESS OF THE TRACK KNOWN SOLUTION

Appendix F presents a summary of the proportion of epochs where it is possible to position as the cutting side angles increases. Here a track precision of 1m is assumed and results are averaged over cutting azimuth and 24 hours.

Incorporating knowledge of the track into the positioning solution provides a substantial benefit for GPS use in cuttings, for example in a 40° cutting a it allows a position with the specified criteria (section 7.1) 85.5% of the time, a substantial improvement over the 58.3% for unassisted positioning. However, this improvement is still insufficient to allow GPS to be used to reliably position trains, since for example in a 60° cutting the proportion of epochs a position is possible is less than 30%, even with the Track Known solution. It is therefore unlikely that GPS by itself could be used as the primary positioning system on a train, even assisted in this manner. This issue will be discussed further in sections 8.2 and 8.3.

8. FURTHER WORK

8.1 MORE REALISTIC MODELLING OF CUTTING SIDES

The current model assumes uniform cutting sides that extend infinitely along the track direction. More sophisticated modelling of the shape of the cutting sides would improve the accuracy of the spreadsheet results.

It would be possible to use a photogrammetric video camera which can distinguish the sky, or a laser scanner mounted on a train at the same height as the GPS receiver to create a model of nearby obstructions as the train runs along the track. The main problem with this is that it may be hard to tell whether identified obstructions will block GPS signals or not.

Another solution to the problem of precise modelling of the sides would be to place GPS receivers on trains and record which satellites are visible at which times. Eventually a database could be built up which would cover the whole railway network for all time periods.

8.2 INCREASING THE NUMBER OF SATELLITES

It would be interesting to expand this study to include the additional satellites of GLONASS and those of Galileo, once it is operational. Including both of these should approximately triple the number of available satellites, allowing a position to be determined in a much higher proportion of epochs. For example, table E.1 shows that in a 70° cutting the mean number of visible satellites is 2.2 (averaged over cutting azimuth and 24 hours) which is insufficient to compute a position. Assuming roughly similar numbers of visible satellites for GLONASS and Galileo we have 6.6 visible satellites, allowing error detection.

It may be possible to increase the coverage using pseudolites, devices of known position that emit GPS-like signals. These could be placed in tunnels and stations to allow positions to be determined in such locations. However, this would mean a much greater requirement for expensive track infrastructure.

8.3 INTEGRATION WITH OTHER SYSTEMS

Due to the requirements of satellite visibility it is unlikely that GPS could be used as a stand-alone positioning system, even utilising a comprehensive track database. There will always be stretches of track where insufficient satellites are visible, not least in tunnels and stations. This loss of position is unacceptable in such a safety-critical application.

The most suitable systems for integration with GPS are either an inertial surveying system or a wheel-mounted odometer. GPS could be used to control the build-up of errors from these sensors and they could cover the periods when GPS was inoperable. However, these systems give the change in position between two epochs, whereas GPS gives the position at each epoch. It is therefore not possible to directly include measurements from either of these in the positioning solution as set up in the spreadsheet – a more sophisticated technique such as a Kalman Filter is required and this is beyond the scope of this project.

9. BIBLIOGRAPHY

ALLAN, A.L., 1997. *Maths for Map Makers, 2nd Edition.* Whittles Publishing, Scotland. 394 pages.

CROSS, P. A., 1984. *Working Paper No. 6, Advanced least squares applied to position-fixing.* University of East London School of Surveying, London. 205 pages.

LEICK, A., 2004. *GPS Satellite Surveying, 3rd Edition.* John Wiley & Sons, Hoboken, New Jersey. 464 pages.

APPENDIX A

COMPARISON OF SPREADSHEET SATELLITE VISIBILITY WITH LEICA SATELLITE AVAILABILITY PROGRAM

A.1 TABLE SHOWING LEICA SATELLITE AVAILABILITY OBSTRUCTION INPUTS

Obstruction Azimuth (°)	Obstruction Elevation Angle (°)		
	30° Cutting	50° Cutting	70° Cutting
0	0.0	0.0	0.0
10	5.7	11.7	25.5
20	11.2	22.2	43.2
30	16.1	30.8	53.9
40	20.4	37.5	60.5
50	23.9	42.4	64.6
60	26.6	45.9	67.2
70	28.5	48.2	68.8
80	29.6	49.6	69.7
90	30.0	50.0	70.0
100	29.6	49.6	69.7
110	28.5	48.2	68.8
120	26.6	45.9	67.2
130	23.9	42.4	64.6
140	20.4	37.5	60.5
150	16.1	30.8	53.9
160	11.2	22.2	43.2
170	5.7	11.7	25.5
180	0.0	0.0	0.0
190	5.7	11.7	25.5
200	11.2	22.2	43.2
210	16.1	30.8	53.9
220	20.4	37.5	60.5
230	23.9	42.4	64.6
240	26.6	45.9	67.2
250	28.5	48.2	68.8
260	29.6	49.6	69.7
270	30.0	50.0	70.0
280	29.6	49.6	69.7
290	28.5	48.2	68.8
300	26.6	45.9	67.2
310	23.9	42.4	64.6
320	20.4	37.5	60.5
330	16.1	30.8	53.9
340	11.2	22.2	43.2
350	5.7	11.7	25.5
360	0.0	0.0	0.0

A.2 TABLE OF RESULTS

	Number of Visible Satellites							
	10° Cutting		30° Cutting		50° Cutting		70° Cutting	
Epoch	Leica	Spreadsheet	Leica	Spreadsheet	Leica	Spreadsheet	Leica	Spreadsheet
00:00	9	9	7	6	3	3	1	2
00:30	9	8	7	7	2	2	2	2
01:00	7	7	5	5	3	3	2	2
01:30	7	8	5	5	3	3	1	1
02:00	8	8	4	4	3	3	1	1
02:30	7	7	5	5	3	3	0	0
03:00	8	8	5	5	4	4	1	1
03:30	8	7	5	5	3	3	1	1
04:00	7	7	4	4	3	3	1	2
04:30	8	7	4	4	3	3	2	2
05:00	8	8	6	6	4	3	2	2
05:30	8	8	7	7	3	3	2	2
06:00	9	9	6	6	5	5	2	2
06:30	10	9	6	6	5	5	2	2
07:00	8	7	6	5	4	3	3	2
07:30	8	8	4	4	3	2	1	1
08:00	8	8	4	5	2	2	1	1
08:30	8	9	6	6	2	2	1	1
09:00	8	9	6	7	2	2	1	1
09:30	8	9	5	6	2	3	1	1
10:00	8	9	7	8	2	2	1	1
10:30	8	9	6	7	3	4	2	2
11:00	8	9	6	7	4	4	2	2
11:30	9	10	7	8	3	4	3	3
12:00	9	10	7	8	4	4	2	2
12:30	8	8	5	6	5	5	2	3
13:00	7	7	5	5	4	4	3	3
13:30	7	7	7	6	5	5	2	2
14:00	8	8	6	6	5	5	2	2
14:30	9	9	7	7	5	6	2	3
15:00	8	8	6	6	4	5	1	2
15:30	7	7	6	6	4	4	1	1
16:00	7	6	6	5	3	3	1	1
16:30	8	8	4	5	3	3	2	2
17:00	9	7	5	5	2	2	2	2
17:30	7	7	6	6	3	3	1	1
18:00	7	7	5	5	5	5	2	2
18:30	7	9	5	5	4	4	2	2
19:00	9	10	5	5	4	4	3	3
19:30	8	9	5	5	2	2	2	2
20:00	8	9	5	5	2	3	1	1
20:30	8	9	7	8	3	3	1	1
21:00	8	8	5	8	3	3	1	1
21:30	9	10	4	4	3	3	1	1
22:00	8	7	5	6	2	2	2	2
22:30	8	8	4	4	2	2	1	1
23:00	8	8	5	5	3	3	1	1
23:30	9	9	6	6	3	3	0	0

A.3 CUTTING ANGLE 10°

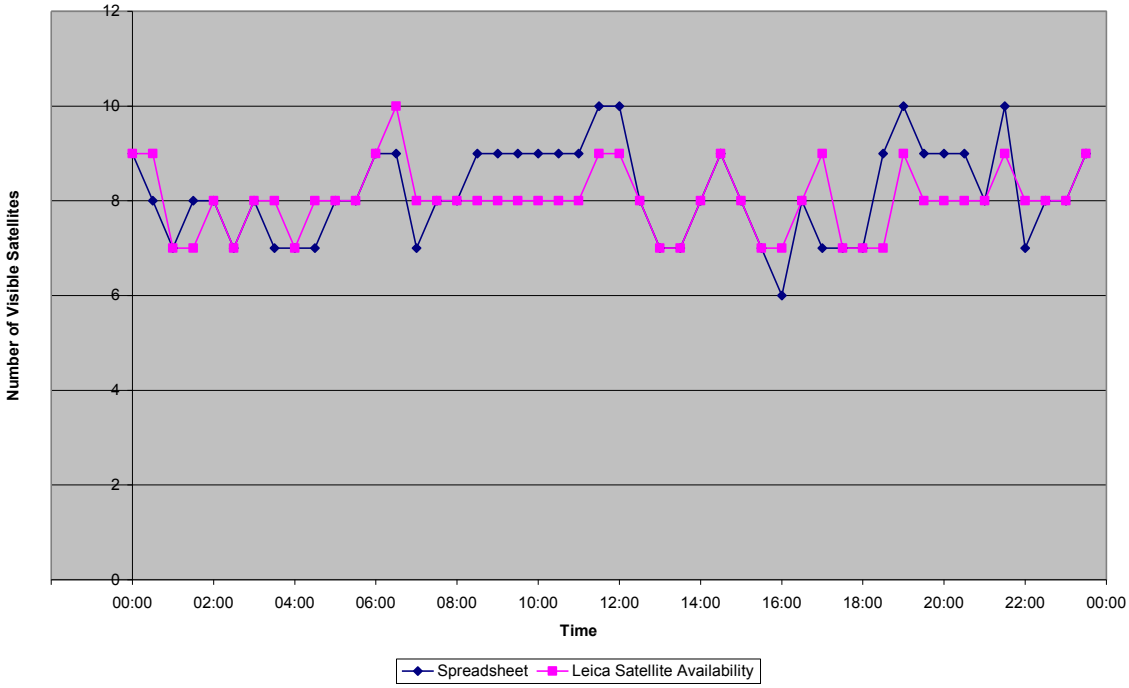

A.4 CUTTING ANGLE 30°

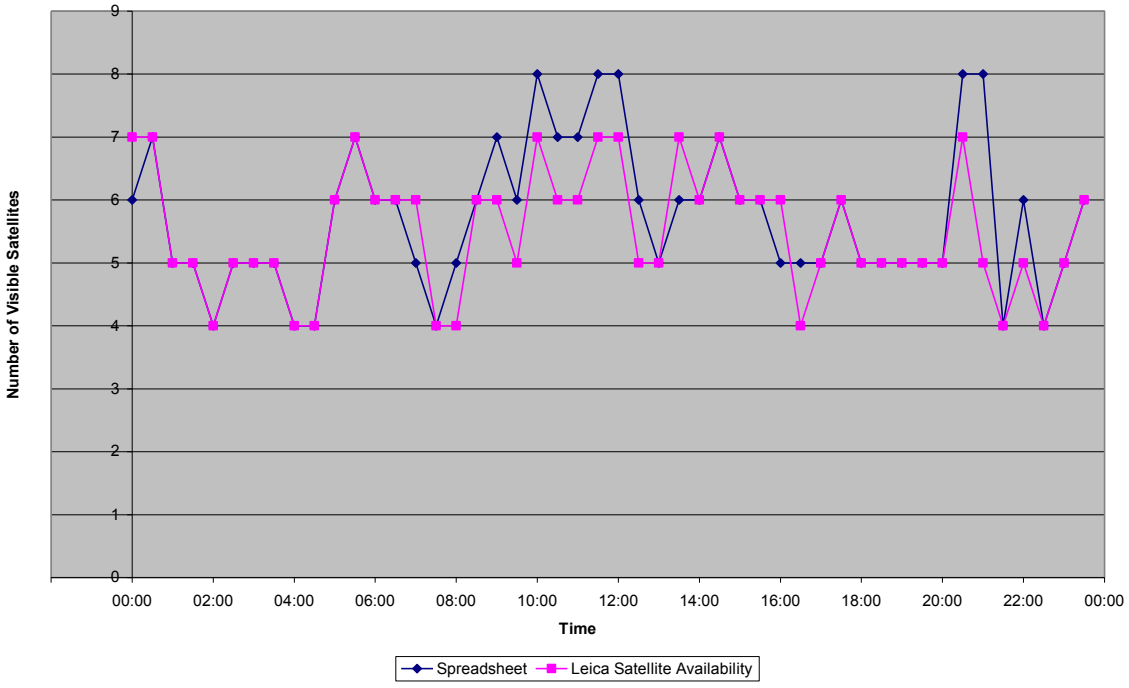

A.5 CUTTING ANGLE 50°

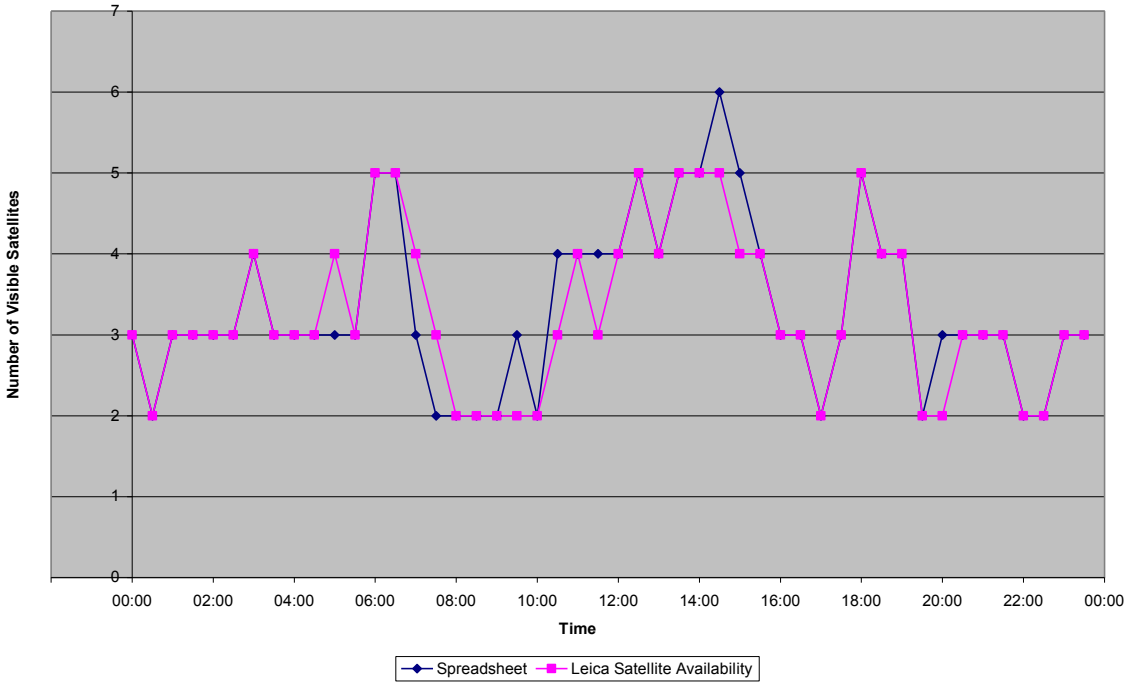

A.6 CUTTING ANGLE 70°

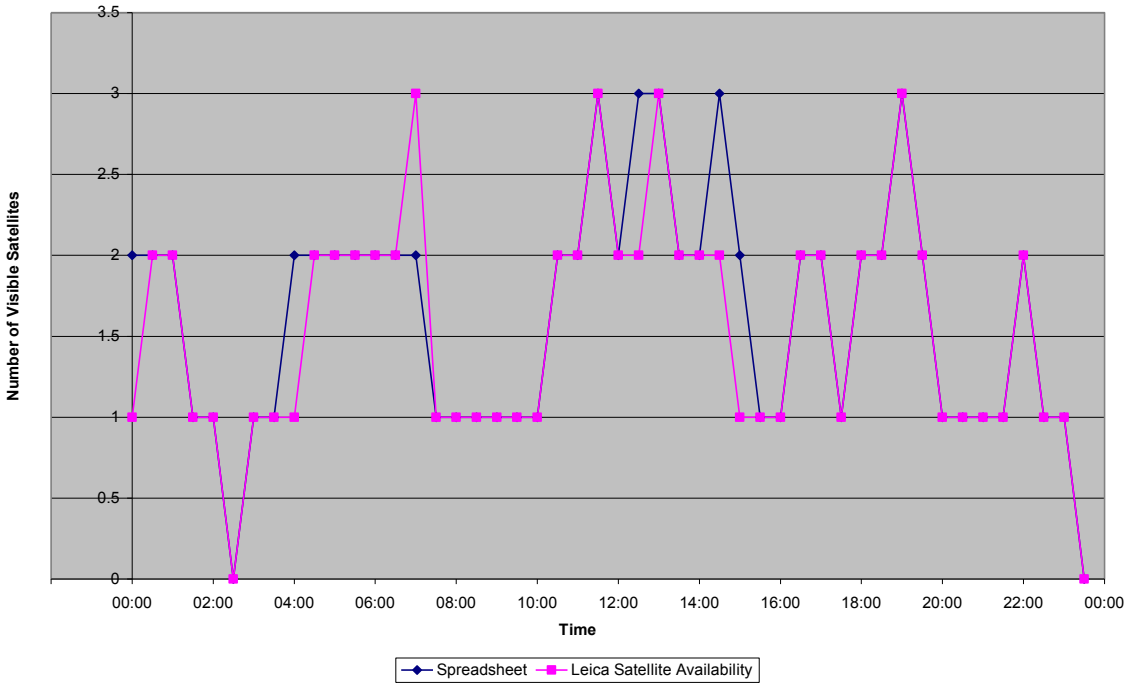

APPENDIX B

ANALYSIS OF THE EFFECT OF CUTTING AZIMUTH

B.1 TABLE SHOWING HOW COMPUTED STATISTICS VARY WITH CUTTING AZIMUTH

Cutting Azimuth (°)	Mean Satellites	% Epochs Error Detection		Mean Improvement					
				σAlong		Max δAlong		% Epochs Error Detection	
		Track Unknown	Track Known	(m)	%	(m)	%	Value	%
0	4.5	34.4	64.6	0.484	16.8	19.462	44.5	30.2	87.9
10	4.4	31.3	64.6	0.565	18.3	24.223	51.7	33.3	106.7
20	4.8	41.7	76.0	0.405	13.8	28.228	51.6	34.4	82.5
30	5.1	50.0	80.2	0.452	15.4	21.028	42.1	30.2	60.4
40	5.3	59.4	86.5	1.048	36.7	31.621	67.0	27.1	45.6
50	5.4	59.4	94.8	1.174	41.3	27.935	61.1	35.4	59.6
60	5.6	71.9	97.9	1.165	41.7	28.687	62.6	26.0	36.2
70	5.6	71.9	97.9	0.949	39.1	28.136	63.1	26.0	36.2
80	5.6	72.9	99.0	0.530	27.3	24.235	63.7	26.0	35.7
90	5.7	72.9	96.9	0.296	17.7	18.784	62.5	24.0	32.9
100	5.6	75.0	96.9	0.251	14.8	11.022	43.9	21.9	29.2
110	5.6	76.0	96.9	0.235	13.1	16.928	49.0	20.8	27.4
120	5.6	74.0	92.7	0.414	19.7	16.477	45.5	18.8	25.4
130	5.5	72.9	89.6	0.535	22.7	23.300	55.5	16.7	22.9
140	5.4	62.5	89.6	0.668	25.6	22.146	54.7	27.1	43.3
150	5.2	57.3	89.6	0.769	28.1	22.734	49.4	32.3	56.4
160	5.0	52.1	83.3	0.684	25.5	22.111	45.5	31.3	60.0
170	4.5	41.7	67.7	0.661	21.9	21.018	43.9	26.0	62.5

B.2 GRAPH OF SATELLITE VISIBILITY VARIATION WITH CUTTING AZIMUTH

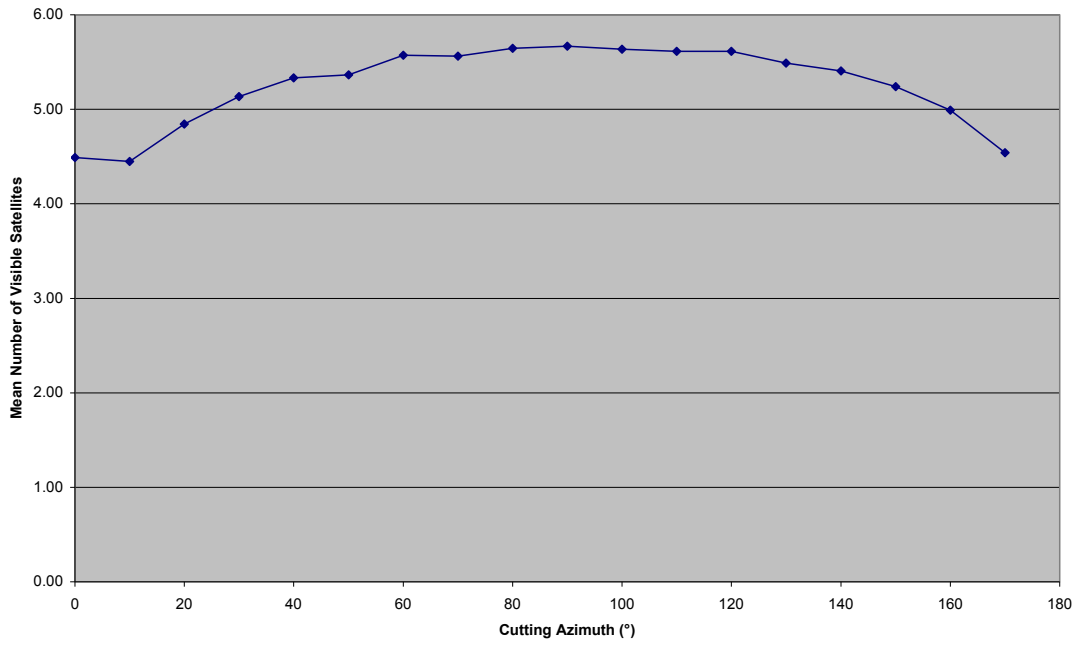

B.3 Graph of Improvement in Proportion of Epochs with Error Detection Variation with Cutting Azimuth

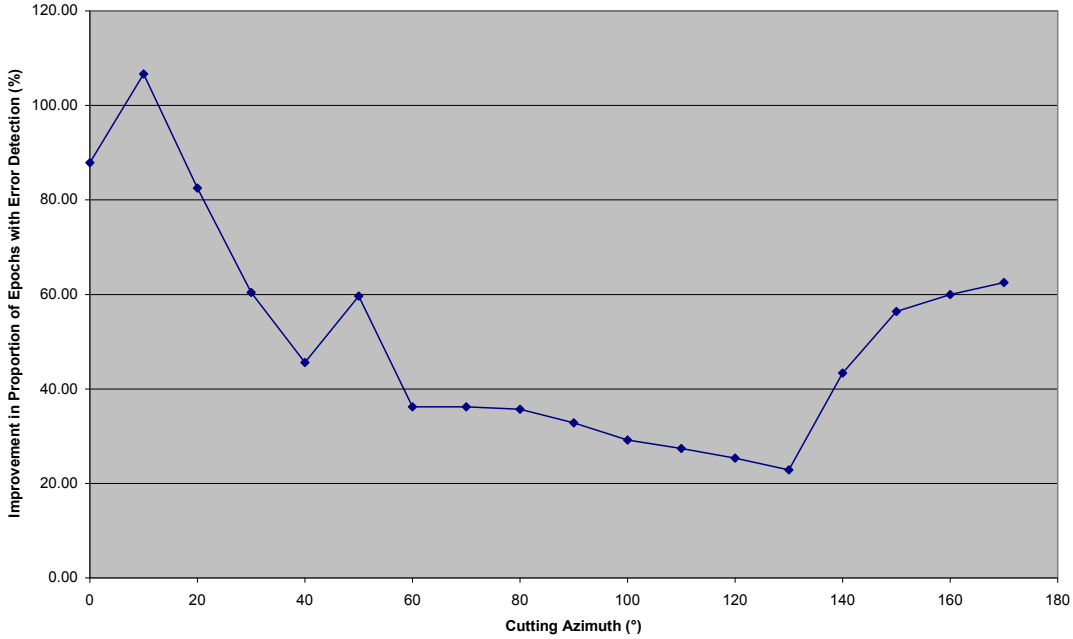

B.4 Graph of Improvement in σ_{Along} Variation with Cutting Azimuth

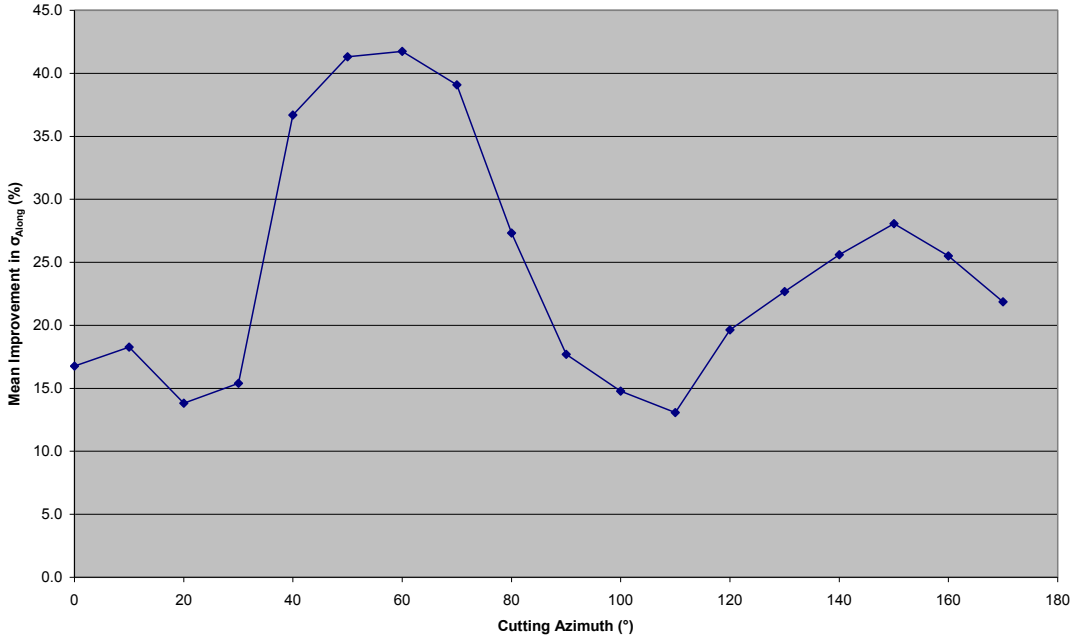

B.5 GRAPH OF IMPROVEMENT IN MAX δ_{Along} VARIATION WITH CUTTING AZIMUTH

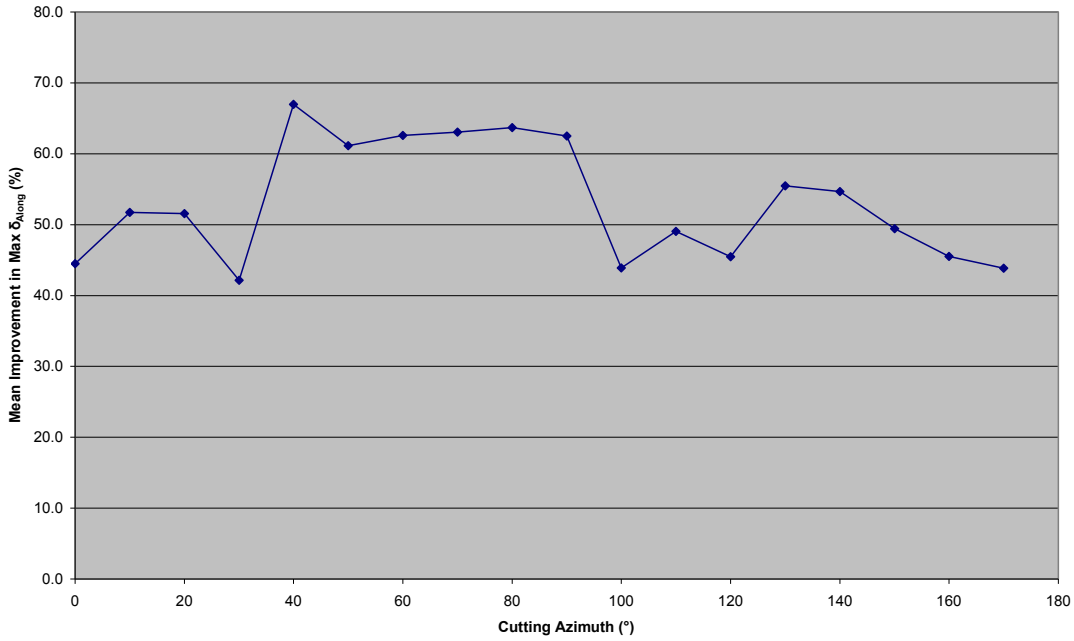

APPENDIX C

ANALYSIS OF THE EFFECT OF LOCATION

C.1 TABLE SHOWING HOW COMPUTED STATISTICS VARY WITH LOCATION FOR 0° CUTTING SLOPE

	Mean Over 24h		
Location	Satellites	$\sigma_{Position}$ (m)	Max $\delta_{Position}$ (m)
SW - Penzance	8.1	2.233	21.931
NE - Aberdeen	8.5	2.322	24.315

C.2 TABLE SHOWING HOW COMPUTED STATISTICS VARY WITH LOCATION FOR 45° CUTTING SLOPE AVERAGED OVER AZIMUTH

				Mean Improvement					
	Mean	% Epochs Error Detection		σAlong		Max δAlong		% Epochs Error Detection	
Location	Satellites	Track Unknown	Track Unknown	(m)	%	(m)	%	Value	%
SW	4.7	44.9	75.3	0.686	24.8	25.603	53.4	30.5	67.9
NE	4.6	39.9	72.1	0.840	27.5	25.412	51.6	32.2	80.7

C.3 GRAPH OF SATELLITE VISIBILITY VARIATION WITH LOCATION FOR 0° CUTTING SLOPE

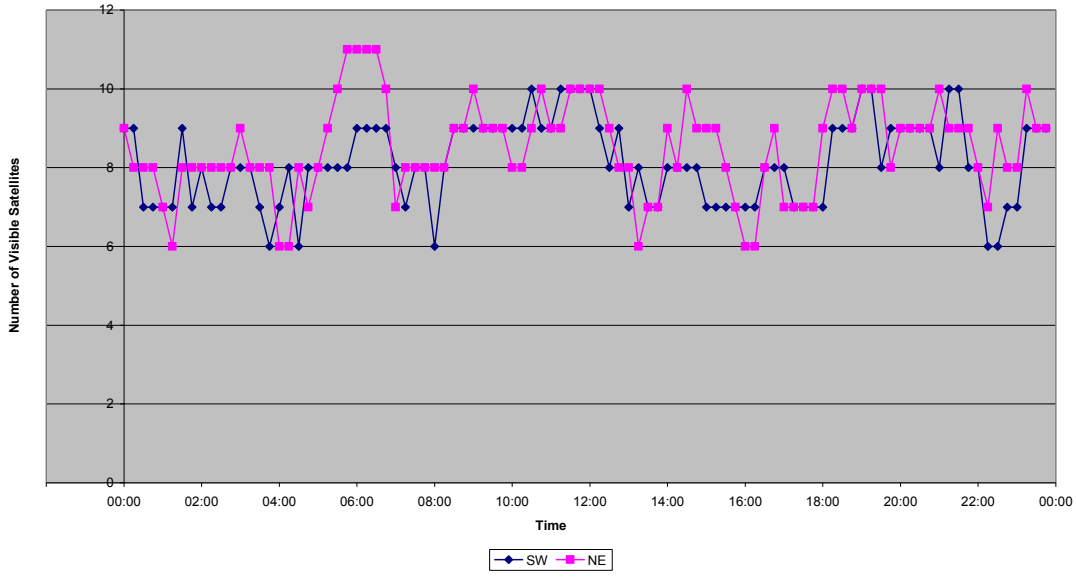

C.4 GRAPH OF $\sigma_{Position}$ VARIATION WITH LOCATION FOR 0° CUTTING SLOPE

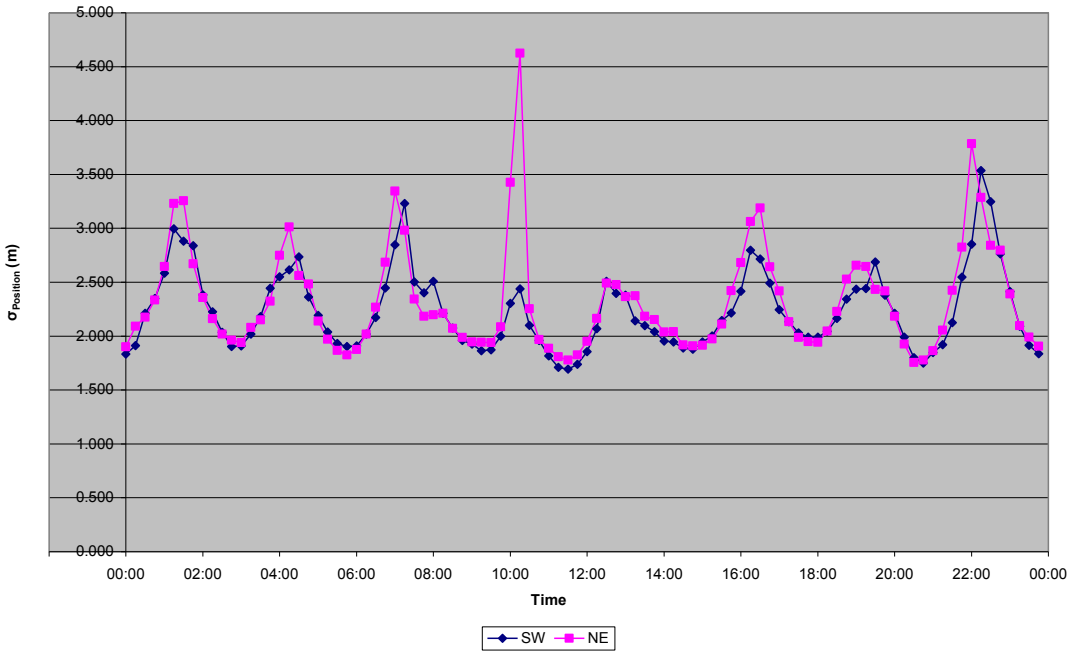

C.5 GRAPH OF MAX $\delta_{Position}$ VARIATION WITH LOCATION

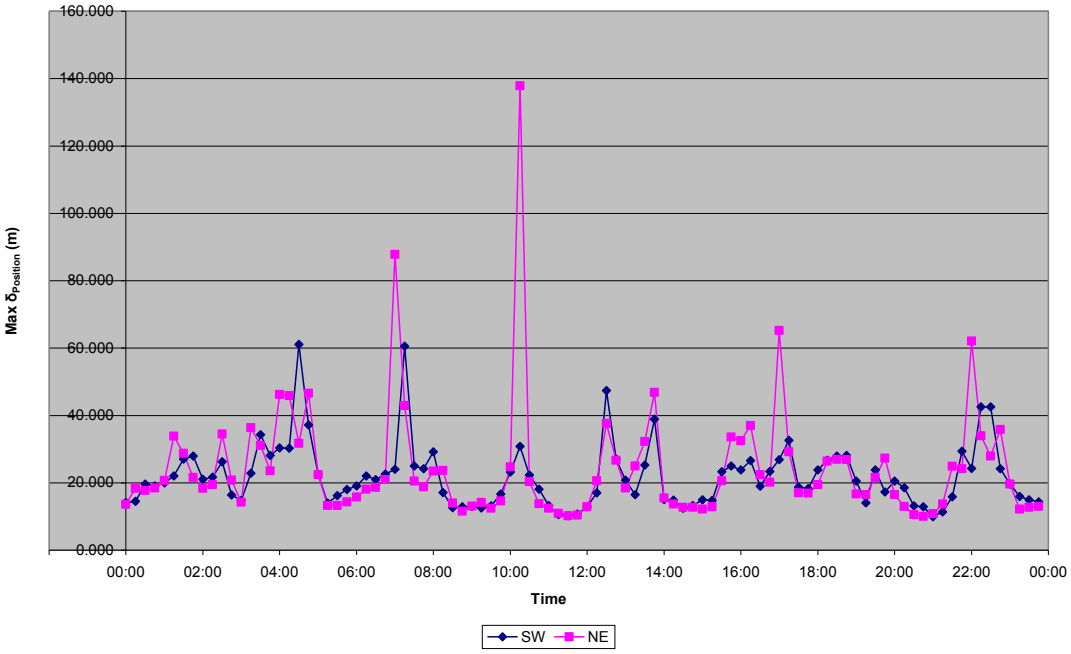

APPENDIX D

ANALYSIS OF THE EFFECT OF TRACK PRECISION

D.1 TABLE SHOWING HOW COMPUTED STATISTICS VARY WITH TRACK PRECISION

			Mean Improvement					
Track Precision σ (m)	% Epochs Error Detection		σAlong		Max δAlong		% Epochs Error Detection	
	Track Unknown	Track Known	(m)	%	(m)	%	Value	%
0.001	44.0	73.4	0.748	25.9	26.009	53.2	29.4	66.8
0.01	44.0	73.3	0.748	25.9	25.971	53.2	29.3	66.6
0.1	44.0	73.3	0.747	25.9	25.968	53.2	29.3	66.6
1	44.0	73.2	0.722	25.1	25.703	52.6	29.2	66.3
5	44.0	71.5	0.463	16.4	21.709	44.7	27.5	62.5
10	44.0	67.9	0.261	9.4	16.819	34.8	23.9	54.2
100	44.0	45.7	0.011	0.4	2.452	5.1	1.7	3.9

D.2 GRAPH OF IMPROVEMENT IN PROPORTION OF EPOCHS WITH ERROR DETECTION VARIATION WITH TRACK PRECISION

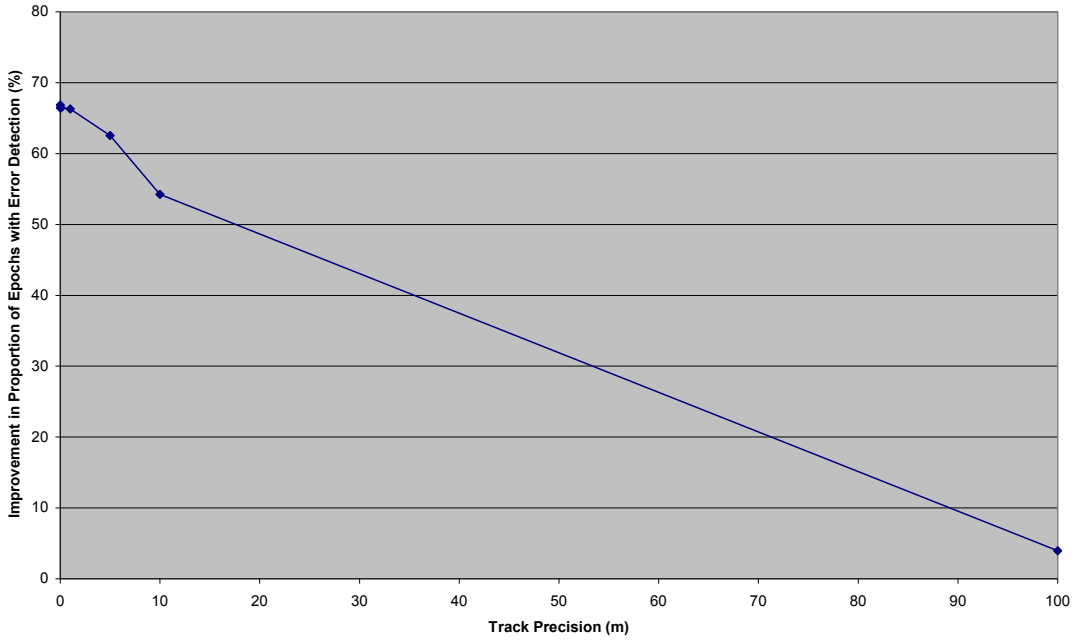

D.3 GRAPH OF IMPROVEMENT IN σ_{Along} VARIATION WITH TRACK PRECISION

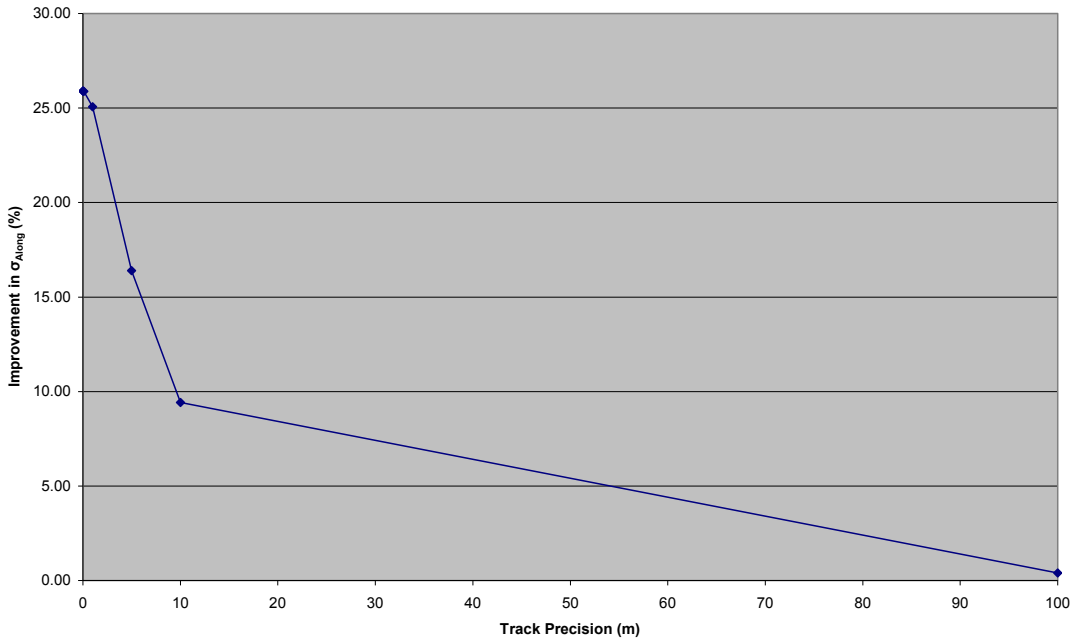

D.4 GRAPH OF IMPROVEMENT IN MAX δ_{Along} VARIATION WITH TRACK PRECISION

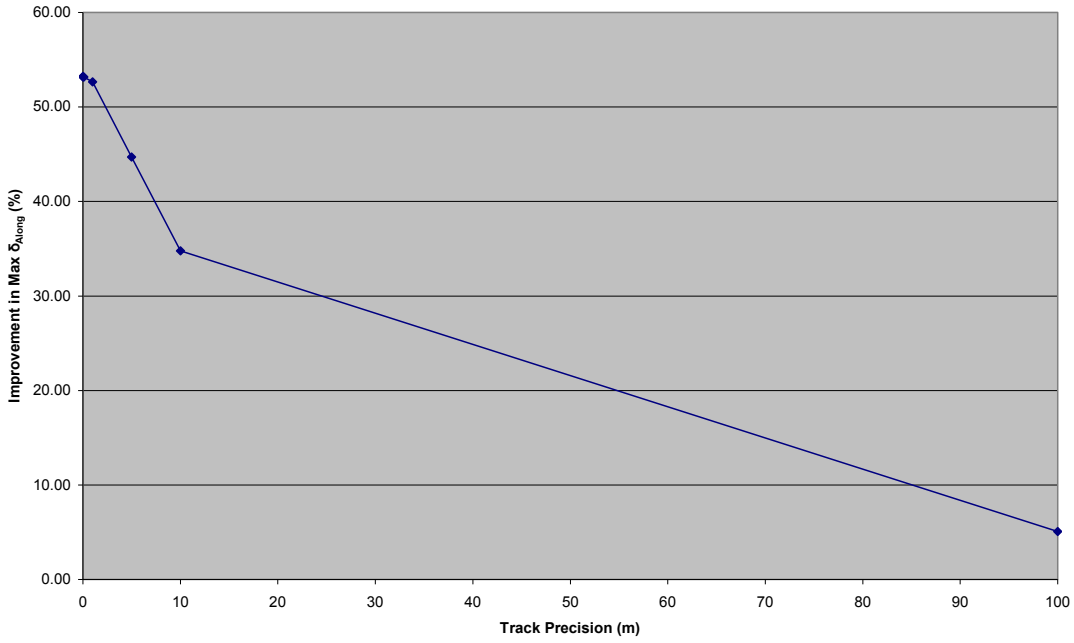

APPENDIX E

ANALYSIS OF THE EFFECT OF CUTTING SIDE ANGLE

E.1 TABLE SHOWING HOW COMPUTED STATISTICS VARY WITH CUTTING SIDE ANGLE

			Mean Improvement					
Cutting Side	% Epochs Error Detection		σAlong		Max δAlong		% Epochs Error Detection	
Angle (°)	Track Unknown	Track Known	(m)	%	(m)	%	Value	%
10	100.0	100.0	0.219	13.3	5.928	35.9	0.0	0.0
20	98.8	99.9	0.256	14.5	9.367	42.4	1.1	1.1
30	86.5	97.6	0.413	19.6	16.452	50.9	11.1	12.9
40	58.3	85.6	0.621	23.9	22.988	53.2	27.3	46.7
50	27.4	57.8	0.860	26.9	32.866	54.1	30.4	110.8
60	7.6	29.4	1.410	35.5	53.701	69.7	21.8	285.2
70	0.5	7.7	2.013	43.1	39.423	58.7	7.2	1383.3
80	0.0	0.4	3.836	59.4	Sat.	Sat.	0.4	Sat.

E.2 GRAPH OF SATELLITE VISIBILITY VARIATION WITH CUTTING SIDE ANGLE

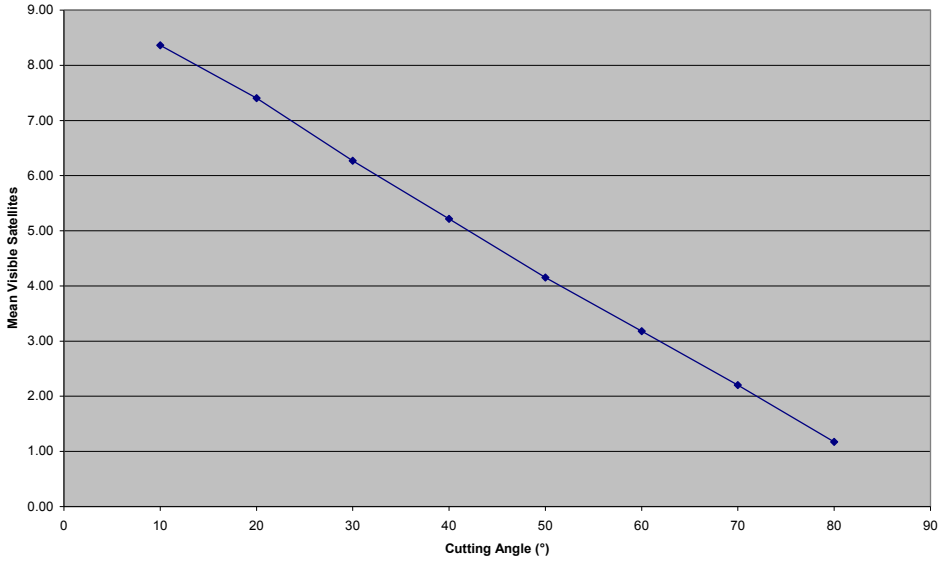

E.3 Graph of Improvement in Proportion of Epochs with Error Detection Variation with Cutting side Angle

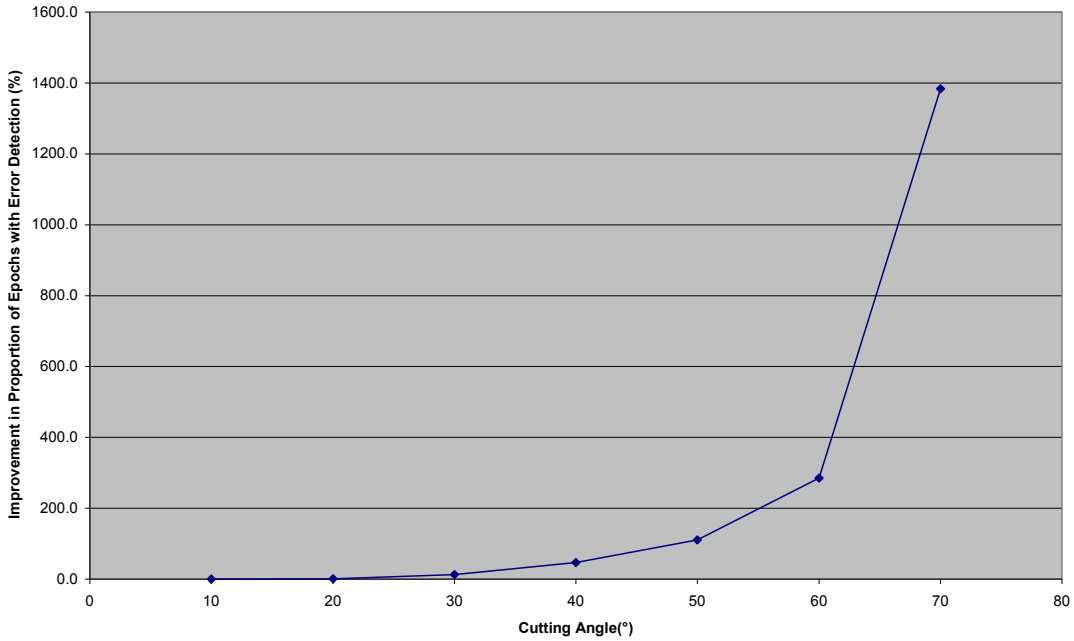

E.4 Graph of Mean Improvement in σ_{Along} Variation with Cutting side Angle

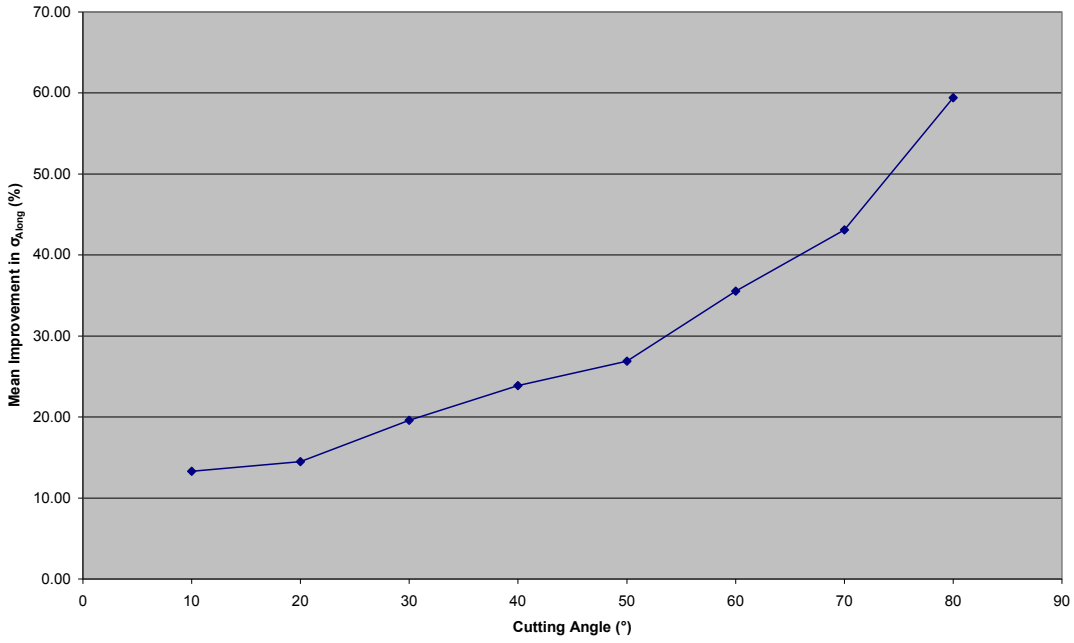

E.5 GRAPH OF MEAN IMPROVEMENT IN MAX δ_{Along} VARIATION WITH CUTTING SIDE ANGLE

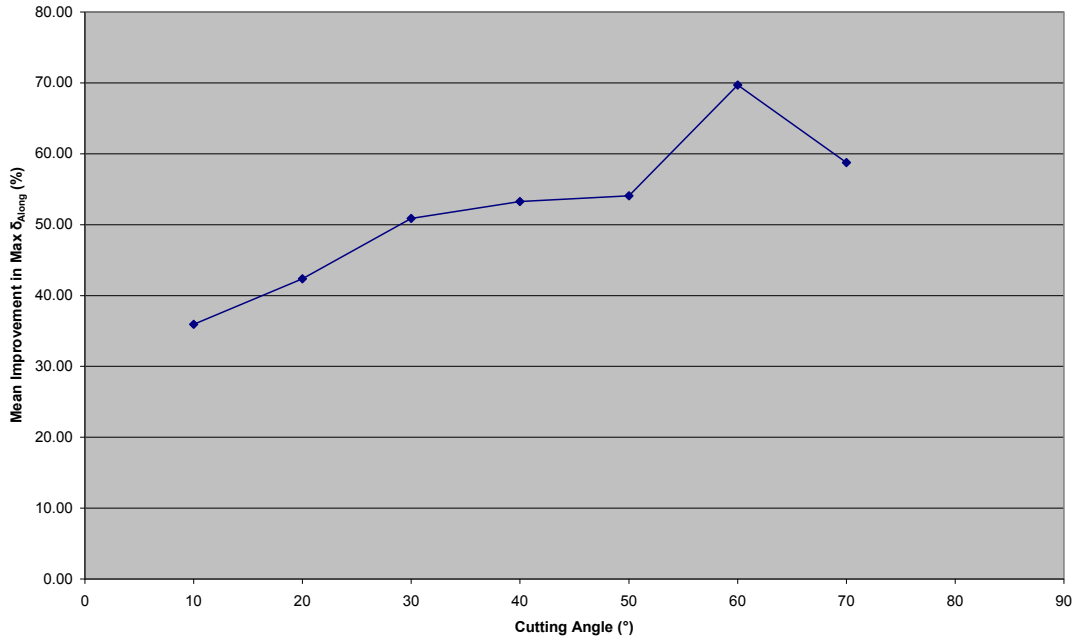

APPENDIX F

ANALYSIS OF THE EFFECTIVENESS OF THE TRACK KNOWN SOLUTION

F.1 TABLE SHOWING HOW PROPORTION OF EPOCHS WITH ERROR DETECTION VARIES WITH CUTTING SIDE ANGLE FOR 1M TRACK PRECISION

			Mean Improvement	
Cutting Side Angle (°)	% Epochs Error Detection		% Epochs Error Detection	
	Track Unknown	Track Known	Value	%
10	100.0	100.0	0.0	0.0
20	98.8	99.9	1.1	1.1
30	86.5	97.6	11.1	12.9
40	58.3	85.6	27.3	46.7
50	27.4	57.8	30.4	110.8
60	7.6	29.4	21.8	285.2
70	0.5	7.7	7.2	1383.3
80	0.0	0.4	0.4	Sat.

F.2 GRAPH OF PROPORTION OF EPOCHS WHERE A POSITION IS POSSIBLE WITH 1M TRACK PRECISION VARIATION WITH CUTTING SIDE ANGLE